



A review on the adsorption mechanism of different organic contaminants by covalent organic framework (COF) from the aquatic environment

Eman Abdelnasser Gendy^{1,2} · Daniel Temitayo Oyekunle¹ · Jerosha Iftikhar¹ · Ali Jawad¹ · Zhuqi Chen¹

Received: 30 June 2021 / Accepted: 13 January 2022 / Published online: 22 February 2022
© The Author(s), under exclusive licence to Springer-Verlag GmbH Germany, part of Springer Nature 2022

Abstract

Recently, covalent organic frameworks (COFs) have gained significant attention as a promising material for the elimination of various organic pollutants due to their distinctive characteristics such as high surface area, adjustable porosity, high removal efficiency, and recyclability. The efficiency and selectivity of COFs depend on the decorated functional group and the pore size of the chemical structure. Hence, this review highlights the adsorption removal mechanism of different organic contaminants such as (pharmaceutical and personal care products, pesticides, dyes, and industrial by-products) by COFs from an aqueous solution. Spectroscopic techniques and theoretical calculation methods are introduced to understand the mechanism of the adsorption process. Also, a comparison between the performance of COFs and other adsorbents was discussed. Furthermore, future research directions and challenges encountered in the removal of organic contaminants by COFs are discussed.

Keywords Adsorption · Covalent organic frameworks · Removal mechanism · Organic contaminants

Introduction

Water is essential for humans and the environment. The great challenge is keeping water as safe and clean as possible (Cabral & health 2010). Among different types of pollutants in water, organic contaminants have attracted attention due to their occurrence at high concentrations in different water sources in the ecosystem (Nde et al. 2018; Nieder et al. 2018). Organic contaminants are present in surface and groundwater, usually from natural origin or indiscriminate discharge of synthetic chemicals into the environment.

Among several major sources of organic contaminants are the industrial production process, human activities, and agriculture (Lv et al. 2019). Organic contaminants are not only found in marine water (Jiang et al. 2014) and surface water (You et al. 2015), but also in the air, soil, sediments (Azzouz & Ballesteros 2012), and landfills. These contaminants constitute a high risk for human health and the ecosystem due to their toxicity, bioaccumulation, mutagenicity, and carcinogenicity (Meffe & de Bustamante 2014, Stuart & Lapworth 2013). With the increasing use of organic chemicals, the potential for contamination of water resources exists. Therefore, it is urgent to evaluate a suitable means of how to eliminate these hazardous contaminants from the environment.

Organic contaminants can be removed naturally for example through the biodegradation of microorganisms but this process is generally very slow. Other removal methods, such as adsorption (Feng et al. 1997; Tan et al. 2017; Xue et al. 2016), precipitation (Peligro et al. 2016), electrochemical oxidation, degradation (Li et al. 2016), ozonation, filtration (Lam et al. 2018), coagulation-flocculation, chlorination, and photocatalytic oxidation are the most common method to capture these contaminants (Al-Shannag et al. 2015). Hence, in past three decades, adsorption has been one of the most distinguished methods due to the simplicity of the

Responsible Editor: Angeles Blanco

✉ Zhuqi Chen
zqchen@hust.edu.cn

¹ Key Laboratory of Material Chemistry for Energy Conversion and Storage, Ministry of Education; Hubei Key Laboratory of Material Chemistry and Service Failure, School of Chemistry and Chemical Engineering, Huazhong University of Science and Technology, Wuhan 430074, People's Republic of China

² Chemistry Department, Faculty of Science, Kafrelsheikh University, El-Geish Street, P.O. Box 33516, Kafrelsheikh, Egypt

system and excellent efficiency with a high removal capacity (up to 99.9%), and low energy consumption compared to several alternative methods (Huang et al. 2017).

The most classical platforms used in the water treatment industry are activated carbon (Schreiber et al. 2006), metal oxides (Nagpal et al. 2019), mesoporous silica (Walcarius & Mercier 2010), and polymers cyclodextrins (Hu et al. 2020b), and chitosan (Heydaripour et al. 2019). The ideal adsorbent is characterized by a large surface area and high porosity with definite adsorption sites. COFs are synthesized with a remarkable porous structure which improves their adsorption capacity.

COFs are a new class of crystalline porous polymer that can be two-dimensional (2D) or three-dimensional (Chen et al. 2020, Fang et al. 2014, Gendy et al. 2021b, Geng et al. 2020b, Huang et al. 2016). They consist of light elements (C, H, O, N, or B atoms) with a strong covalent bond. Due to the exceptional properties and the various functional group, COFs have become more attractive due to their (1) low density; (2) large surface area; (3) high crystalline; (4) tunable ultrahigh porosity; (5) facile tailored functionality; (6) versatile covalent combination; (7) high thermal and mechanical stability; (8) selectivity of the interaction sites for definite adsorbate; (9) changeable pore structure (pore volumes, uniform pore size); (10) high internal surface area; (11) elaborate control of geometry. These attributes encourage the application of COFs in different industrial and technological fields (Das et al. 2017) including adsorption, separation, catalysis, and sensing (Song et al. 2019).

More than 33,306 scientific articles titled COFs and around 4,525 COFs/organic contaminants have been viewed in the science database search (January 2010–January 2022). As shown in Fig. 1, the number of publications on COFs and their application in the removal of organic contaminants is increased gradually every year, specifically from 2018 to 2021, indicating that COFs are currently the promising research trend (Bagheri et al. 2021, Bisbey & Dichtel 2017,

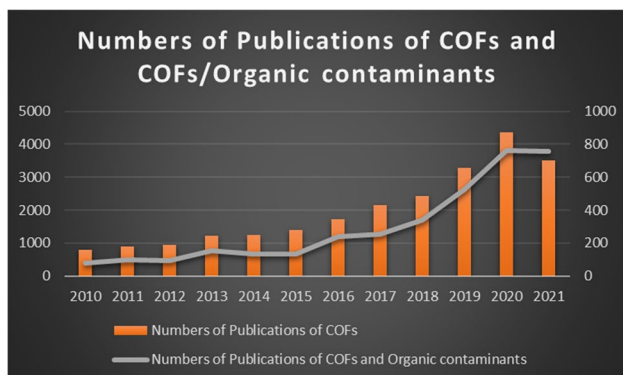


Fig. 1 Number of publications on COFs and COFs/Organic contaminants from 2010 to 2022 based on the database of “web of Science”

Cao et al. 2019, Das et al. 2017, Gendy et al. 2021a, Geng et al. 2020a, Lv et al. 2019, Song et al. 2019, Wang et al. 2017).

Herein, this review discusses the interaction mechanism between the adsorbate and the adsorbent. The elimination of organic pollutants by COFs and their selectivity are evaluated and reviewed. The performance of COFs in comparison to other platforms has also been mentioned. This review paper discusses the removal mechanism of organic pollutants such as (pharmaceutical and personal care products, pesticides, dyes, and industrial by-products) by covalent organic frameworks based on the chemical structure and functional group. In addition, the selectivity and efficiency of COFs under the different environmental conditions (pH, temperature, contact time, etc.) were elucidated.

Removal of organic contaminants by COFs and their adsorption mechanism

Removal of organic contaminants by COFs

COF-based materials are used as a superior platform for the removal of organic pollutants from aqueous solutions. Other parameters influence the adsorption performance of these contaminants by COFs such as pH, concentration, temperature, adsorption kinetics, contact time, and recyclability. The present section focuses on the recent progress and investigations of removing organic water pollutants based on adsorption by COFs. However, some reviews have also been reported dealing with the adsorption process. We hope this section would be a kind extension of such inclusive reviews. The information was collected by categorizing organic pollutants, such as pharmaceuticals, pesticides, dyes, and industrial by-products. The reported information is summarized and documented in Tables 1, 2, 3 and 4.

Pharmaceutical and personal care products (PPCPs) contaminants

PPCPs act as the most significant types of organic pollutants. These chemicals are widespread in the environment due to the constant consumption of medicines, cosmetics, and household chemicals in modern societies. The lack of effective protocols for decontamination causes precipitation and accumulation of these pollutants in the aquatic environment (Bu et al. 2013). Several studies have strongly proposed that the existence of these contaminants at very low doses is dangerous and harmful for humans and the environment in the long term. Due to its various effects and serious risks on marine species and the health of humans, PPCPs have attracted considerable attention and effective elimination is essential according to current water treatment protocols.

Table 1 Pharmaceutical contaminants adsorption data for reported COF-based materials

COF-based materials	Optimum pH	Selectivity	Target	Maximum adsorption capacity (mg g ⁻¹)	Initial concentration L ⁻¹	Time of equilibrium	Reusability	Reference
MCOF-2	5	DS	DS	565	200	20 min	Methanol/ 5 cycles	(Huang et al. 2019)
TpBD-(CF₃)₂	2	IBU DS ACE Ampicillin	IBU	119	100	60 min	Isopropanol/NA	(Mellah et al. 2018)
TPB-DMTP-COF	7	SMT	SMT	209	200	80 min	Methanol, ethanol, or THF /4 cycles NA	(Zhuang et al. 2020b) (Wang et al. 2018b)
β-cyclodextrin COF	NA	BPA Acridine orange IBU 4-Nonyl phenol NPX	BPA IBU NPX	99% 98% 78%	630 135 120	10 min		
TAB-DVA-COF	10	BPA BPB IBU BPC CIP NPX SMZ SIZ SMT IDM ENX KT	IDM NPX DCF IBU KT	25% 20% 20% 23% 30%	1000	NA	NA	(Hao et al. 2019)
COF-SO₃H	10	IBU NPX BPA BPB BPC CIP IDM ENX KT SMZ SIZ SMT	IDM NPX DCF IBU KT	95% 59% 94% 48% 57%	1000	30 min	NA/ 4 cycles	(Hao et al. 2019)

Table 1 (continued)

COF-based materials	Optimum pH	Selectivity	Target	Maximum adsorption capacity (mg g ⁻¹)	Initial concentration mg L ⁻¹	Time of equilibrium	Reusability	Reference
Fe ₃ O ₄ @COF(TpBD)@Au-MPS	5	ENX	ENO	8.52	10	25 min	NA	(Wen et al. 2020)
		DAN	OFL	9.28				
		ORB	CIP	7.34				
		OFL	DAN	7.24				
		ENO	ENRO	7.01				
CIP	ORB	8.76						
Magnetic TPB-DMTP-COF	6	DS	DS	109	200	80 min 50 min	NA	(Zhuang et al. 2020a)
		SMT	SMT	113.2				
NCCT	8	CTX	CTX	309.3	400	8 h	0.1 M NaOH/6 cycles	(Li et al. 2020b)
		TC	TC	388.52				

Different methods have been used for the capture of PPCPs from the aquatic environment, including adsorption (Wang & Wang 2019, Zhuang et al. 2018), microbial degradation (Wang et al. 2018a) Fenton-like oxidation (Liu et al. 2018b), ozonation (Wang & Bai 2017), ionizing radiation (Zhuang & Wang 2019), and other advanced oxidation processes AOPs (Wang & Wang 2018). Adsorption is a promising method due to its low cost and high efficiency and energy consideration compared to other methods. In addition, it avoids poisonous degradation products and resistance genes/bacteria, which may produce secondary contamination to the environment. Many pharmaceutical drugs have been commonly used for human care and animal husbandry (Xu et al. 2017; Yang et al. 2017)

PPCPs are categorized depending on purposes and their features: (1) Antibiotics: sulfamethoxazole (SMZ), sulfafurazole (SIZ), sulfamethazine (SMT), enrofloxacin (ENX), ampicillin, danofloxacin (DAN), ofloxacin (OFL), cefotaxime (CTX), orbifloxacin (ORB), ciprofloxacin (CIP), tetracycline (TC), enoxacin (ENO); (2) anti-inflammatory drug: ibuprofen (IBU), diclofenac sodium (DS), ketoprofen (KT), indomethacin (IDM), naproxen (NPX); (3) Analgesic: acetaminophen (ACE). There is a shortage of removal of other types of PPCPs like (anti-cancer, anti-bacterial, anti-psychotic, asthma drug, etc.) by using COFs. Therefore, it is necessary to show the removal efficiency of these kinds of contaminants by COFs.

Antibiotics

Antibiotics are a kind of pharmaceutical drug that is used in the treatment of human and veterinary medicine. Sulfonamides describe a class of drugs containing the sulfanilamide structure such as sulfamethoxazole, sulfafurazole, and sulfamethazine. So far, TPB-DMTP -COF showed q_{max} value of 209 mg g⁻¹ for sulfamethoxazole capture from the water. The high adsorption quantity of TPB -DMTP COF was due to large surface area = 2115 m²/g, large channel ~3.3 nm, high crystallinity. TPB -DMTP COF also showed a higher adsorption capacity for SMT than TAB-DVA-COF and COF-SO₃H (Zhuang et al. 2020b). Fast adsorption equilibrium time (80 min), and good reusability, it was regenerated by THF, ethanol, and methanol, which is feasible and more economical in successive with an even after four adsorption-desorption cycles (Zhuang et al. 2020b). Also, the magnetic TPB -DMTP COF was tested for sulfamethoxazole and showed q_{max} value of 113.2 mg g⁻¹ with a faster equilibrium time (50 min) (Zhuang et al. 2020a).

Fluoroquinolones (FQs) are a significant class of synthetic antibiotics and the third-largest kind consumed in the global market. FQs are derivatives of fluorinated piperazine of nalidixic acid which contain a fluorine atom at the C-6 position and a piperazinyl at the C-7 position. Thus,

Table 2 Pesticide contaminants adsorption data for reported COF-based materials

COF-based materials	Optimum pH	Selectivity	Target	Maximum adsorption capacity (mg g ⁻¹)	Initial concentration mg L ⁻¹	Time of equilibrium	Reusability solvent/ number of cycles	Reference
NH ₂ @COF	4	Imidacloprid	Dicamba	14	0.1	25 min	NA/ 6 cycles	(Ji et al. 2019b)
		tsumacide	2,4,5 T	13				
		Cyhalothrin	2,4 DP	12,5				
		2,4 DP	2,4 D	12				
		2,4 D	4-CPA	12				
		4-CPA	MCPA					
		Dicamba						
		Gentamycin						
		2,4,5 T						
		2,4 DP						
vinyl covalent organic framework (COF)	4	Imidacloprid	Imidacloprid	12.5	0.1	NA	NA	(Ji et al. 2019b)
		Tsumacide	tsumacide	12				
		Cyhalothrin	Cyhalothrin	11,7				
		2,4 DP						
		2,4 D						
		4-CPA						
		MCPA						
		Dicamba						
		Gentamycin						
		2,4,5 T						
DAAQ-TFP	7	Chlorophenols	PAEs	82.8–97.5%	0.16	NA	Acetonitrile/ 30 cycles	(Song et al. 2018)
		PAEs	Bus					
		Bus						
		PUHs						
		EDCs						
		Methomyl						
		Aldicarb						
		Carbaryl						
		Sulfoxide aldicarb						
		Carbofuran						
Fe ₃ O ₄ @SiO ₂ -NH ₂ @COFs	6	Methomyl	Methomyl	> 97%	1000	5 min	Acetone / 10 cycles	(Li et al. 2020a)
		Aldicarb	Aldicarb					
		Carbaryl	Carbaryl					
		Sulfoxide aldicarb	Sulfoxide aldicarb					
		Carbofuran	Carbofuran					
		Sulfone aldicarb	Sulfone aldicarb					
		3-OH carbofuran	3-OH carbofuran					
		Imidacloprid	Imidacloprid					
		Acetamiprid	Acetamiprid					
		Methamidophos	Methamidophos					
Malathion	Malathion							
Dimethoate	Dimethoate							
Diazinon	Diazinon							
Phorate	Phorate							
Thiamethoxam	Thiamethoxam							

small dye molecule methylene blue, achieving a maximum adsorption capacity of 1691 mg g⁻¹ (Zhu et al. 2017).

Table 3 Organic dyes adsorption data for reported COF-based materials

COF-based materials	Optimum pH	Selectivity	Target	Maximum adsorption capacity (mg g ⁻¹)	Initial concentration mg L ⁻¹	Time of equilibrium	Reusability solvent/ number of cycles	Reference
CTF	7	RhB brilliant red X-3B direct scarlet 4BS	RhB	565	191.6	55 min	Ethanol / 4 cycles	(Wang et al. 2014b)
COF-TzDBd	6	CV BG MB AR	CV BG	307 276	350	15 min	Ethanol and 0.1 HCl % / 5 cycles	(Li et al. 2019a)
TPT-DMBD-COF	10	MEB	MEB	279.5	100	60 min	Ethanol and 0.1 mM HCl % / 5 cycles	(Huo 2019)
benzodiazole-COF	3, 11	MO MB acid magenta CV	MO MB	256, 185	500	NA	NaBr/ 5 cycles	(Xu et al. 2020)
TS-COF-2	NA	MEB RhB CR	MEB	1691	100	10 min	Ethanol / 4cycles	(Zhu et al. 2017)
BTT-TAPT-COF	2	4-nitrophenol 3-nitrophenol	IC	547.33	100	120 min	1 M NaOH/ 5 cycles	(Pan et al. 2020)
PC-COF	NA	Iodine MO AG DFBM IC AR-27	MO AG DFBM IC AR-27	> 97%	2.1 X 10 ⁻⁴ M 1.1 X 10 ⁻⁴ M 1.6 X 10 ⁻⁴ M 1.6 X 10 ⁻⁴ M 1.6 X 10 ⁻⁴ M	30 min	NA	(Yu et al. 2016)
Cationic EB-COF:Br		RB MB DMPD MO FS PP NR CA NA	RB MB DMPD MO FS PP NR CA NA	99.6% 99.2% 98.1% 91.2% 87.2% 84.9% 74.4% 22.3% 15.7%	5 X 10 ⁻⁵ M	NA	NaBr/ 6 cycles	(Zhang et al. 2018b)

NA; not available

Table 4 Industrial organic contaminants adsorption data for reported COF-based materials

COF-based materials	Optimum pH	Selectivity	Target	Maximum adsorption capacity (mg g ⁻¹)	Initial concentration mg L ⁻¹	Time of equilibrium	Reusability solvent/ number of cycles	Reference
CTF	NAPH=10 2-NAOL=9 2-NS=3 1-NALA=10 DNB=10 MDNP=4 BEN=10 BS=3 TNB=10	BEN PHOL BEN PHOL AN BS NB DNB TNB MDNP NAPH 2-NAOL 1-NALA 2-NS	NAPH 2-NAOL 2-NS 1-NALA DNB MDNP BEN BS TNB MDNP NAPH 2-NAOL 1-NALA 2-NS	NA	1.3 X 10 ⁻² M	NB=100 min	NA	(Liu et al. 2012)
DhaTab-PBA	9	Resorcinol Hydroquinone Phenol Toluene Catechol chlorobenzene aniline	Catechol	160	1100	40 min	10 mM PBS /5 cycles	(Ji et al. 2019a)
100%[N ₃]-COF	7	PFOA PFOS GenX	Gen X	56%	1000	30 min	NA	(Ji et al. 2018)
75%[N ₃]-COF	7	PFOA PFOS GenX	GenX	70%	1000	30 min	NA	(Ji et al. 2018)
50%[N ₃]-COF	7	PFOA PFOS GenX	GenX	83%	1000	30 min	NA	(Ji et al. 2018)
28%[N ₃]-COF	7	PFOA PFOS GenX	GenX	90%	1000	30 min	Methanol / 3 cycles	(Ji et al. 2018)
20%[N ₃]-COF	7	PFOA PFOS GenX	GenX	97%	1000	30 min	NA	(Ji et al. 2018)
10%[N ₃]-COF	7	PFOA PFOS GenX	GenX	94%	1000	30 min	NA	(Ji et al. 2018)
NA; not available								

the progress of an efficient platform for this class of antibiotics is of principal significance. ENX, ENO, OFL, ORB, DAN, and CIP are examples of FQs. COF-based material ($\text{Fe}_3\text{O}_4@\text{COF}(\text{TpBD})@\text{Au-MPS}$) showed a higher affinity to FQs compared to other similar COF/COF-based materials ($\text{Fe}_3\text{O}_4@\text{COF}(\text{TpBD})$, TAB-DVA-COF and COF- SO_3H for ENX and CIP. $\text{Fe}_3\text{O}_4@\text{COF}(\text{TpBD})@\text{Au-MPS}$ exhibited good selectivity toward ENRO, ENX, DAN, ORB, OFL, ENO, and CIP with maximum extraction capacity 8.52, 9.28, 7.34, 7.24, 7.01, and 8.76 mg g^{-1} , respectively at $\text{pH}=5$ (Table 1). Two dynamic adsorption models (first pseudo-order and second pseudo-order) were used to simulate the control mechanism of the adsorption process with equilibrium time = 25 min (Wen et al. 2020).

Cefotaxime is an antibiotic for the treatment of Gram bacterial infections (Rochon et al. 2019) and tetracycline is the second-largest consumption of antibiotics for the treatment of animals (Khodadadi et al. 2018). NiFe_2O_4 -COF-chitosan-terephthalaldehyde nanocomposites film (NCCT) was used as a potential platform for the removal of cefotaxime and tetracycline with $q_{\text{max}} = 309.26$ and 388.52 mg g^{-1} , respectively. It was regenerated by 0.1 M NaOH after six adsorption–desorption cycles (Li et al. 2020b).

Anti-inflammatory

There is widespread use of anti-inflammatory drugs for animal husbandry and human treatment such as ibuprofen, diclofenac sodium, ketoprofen, indomethacin, and naproxen. Widely used non-steroidal anti-inflammatory drugs have gained increased global awareness due to their frequent detection in the water. Advanced oxidation processes are effective for the removal of diclofenac sodium from wastewater. However, there are drawbacks such as the production of more toxic secondary contaminants, and the techniques are hard to carry out on a large scale. Therefore, the adsorption process is an efficient alternative for capturing diclofenac sodium from wastewater (Xu et al. 2017).

Huang et al. showed magnetic covalent organic frameworks MCOF-2 for capturing diclofenac sodium with $q_{\text{max}} = 565 \text{ mg g}^{-1}$. High adsorption capacity can be explained by high surface areas, proper pore size, good thermal/chemical stability, and separation ease. It was noted that pH solution is effective on the status of the adsorbate and absorbent. The pK_a of diclofenac sodium is 4.2, suggesting that the negative form was dominated at $\text{pH} > 4.2$. Around $\text{pH} = 7$, the charge on the surface of MCOFs -2 shifted from positive to negative. MCOF-2 still had a large capture capacity towards diclofenac sodium when the pH is > 7 . The quantity of diclofenac sodium adsorbed was affected by adding the salt; it was decreased, especially after adding CaCl_2 . The strong competition of cations (Ca^{2+} and Na^+)

in occupying the active sites for diclofenac sodium uptake can be explained by this result. The pseudo-second-order kinetic model could well explain the adsorption process of MCOF-2. Equilibrium of adsorption was attained 20 min for diclofenac sodium and showed good regeneration by methanol after five adsorption–desorption cycles (Huang et al. 2019). Moreover, magnetic TPB –DMTP COF showed q_{max} value of 209 mg g^{-1} for adsorption diclofenac sodium with equilibrium time (80 min) (Zhuang et al. 2020a).

Ibuprofen is a non-steroidal anti-inflammatory drug used for medical treatment for humans and animals (Davarnejad et al. 2018; Kråkström et al. 2021; Oba et al. 2021; Silva et al. 2020). The presence of IBU in nature can have negative effects on living organisms. It can threaten human life and the health of natural habitats. Therefore, the researchers are still discovering ways to remove IBU from water or decrease its presence to a minimum (Davarnejad et al. 2018). IBU is among the most commonly used active medication components in the world ambient surveillance studies. IBU is the second most popular observed drinking water in high concentrations ($> 1 \text{ ppb}$) due to the great consumption of IBU allied with the low efficiency of capture/degradation of traditional water treatment processes. Despite the present lack of organization proper quantity of IBU in different water types, significant efforts are directed from the scientific community to monitor them, eliminate, and/or degrade them.

Mellah et al. reported $\text{TpBD}-(\text{CF}_3)_2$ exhibited high adsorption and selectivity toward ibuprofen among other hydrophilic pharmaceutical contaminants (diclofenac sodium, ampicillin, and acetaminophen) with 119 mg g^{-1} at $\text{pH} = 2$. The large surface area of $870 \text{ m}^2 \text{ g}^{-1}$ and the molecular size of IBU is suitable for entry within the pores of these COF which contributed to increasing adsorption capacity compare to BiOCl microsphere and activated carbons (see Table 6). The affinity order of $\text{TpBD}-(\text{CF}_3)_2$ for removing these contaminants is ibuprofen $>$ acetaminophen $>$ ampicillin due to acetaminophen being slightly close to the size of ibuprofen, whereas ampicillin is slightly larger. The carboxylic acid moiety of Ibuprofen plays a crucial role in drug capture. The adsorption capacity decreased by increasing pH, q_{max} value at $\text{pH} = 2$ and $\text{pH} = 6–7$ ibuprofen is partially negatively charged after $\text{pH} = 7$ the q_{max} value decrease. The kinetic curve presents that equilibrium was attained at 60 min and regenerated by isopropanol (Mellah et al. 2018).

Wang et al. also showed β -cyclodextrin (β -CD) for removal of ibuprofen with an efficiency of 79%. β -CD COF is a hydrophobic cavity guiding molecular-specific recognitions. β -CD COF is synthesized with heptakis (6-amino-6-deoxy)- β -CD and terephthalaldehyde in green solvents of water and ethanol at room temperature. The β -CD COF possesses a larger surface area of $108.2 \text{ m}^2 \text{ g}^{-1}$, a more uniform pore size of $0.332 \text{ cm}^3 \text{ g}^{-1}$, and higher thermal stability at $235.6 \text{ }^\circ\text{C}$ than the non-crystalline β -CD polymer.

Bisphenol A, acridine orange, ibuprofen, 4-nonyl phenol, and (S)-naproxen are tested to show the selectivity of β -CD COF to these contaminants, it was observed that β -CD COF adsorbed bisphenol, ibuprofen, and naproxen with adsorption removal percentage 99, 78, 98 and 98% at 10 min (Wang et al. 2018b).

A varying degree of SO_3H functionalized was incorporated for pharmaceuticals and PPCPs removal by Hao et al. COF- SO_3H was synthesized by presenting sulfonic acid polar functionalities through a simplistic solvothermal method. COF- SO_3H showed a strong affinity for the diclofenac with the maximum adsorption quantities 770 mg g^{-1} , which was evaluated 1.5 times higher than that of commercial active carbon, and graphene oxide, while $\text{SO}_3\text{-UiO-66}$ was evaluated three times higher than these adsorbents. It was also found that COF- SO_3H possess an affinity for personal care products (PPCPs) ibuprofen, diclofenac sodium, ketoprofen, indomethacin, and naproxen of initial concentration [1 g L^{-1}] with removal efficiency 95%, 94%, 59%, 57%, and 48% respectively, while TAB-DVA-COF showed removal efficiency of ibuprofen, diclofenac sodium, ketoprofen, indomethacin, and naproxen 25%, 20%, 20%, 23%, and 30% with initial concentration [1 g L^{-1}]. COF- SO_3H showed good recyclability after four-time (Table 1) and showed excellent recovery after the first two cycles (Hao et al. 2019).

Pesticides

Pesticides are commonly used around the world to control insect pests from a healthy crop. They are a broad spectrum of chemicals and mixtures of organic used to stop plant diseases, pests, and weeds and to improve and maintain the high quality of food products (Lushchak et al. 2018, Rajmohan et al. 2020, Гусак & Луцк 2018). It includes plant growth regulators, fungicides, insecticides, etc. However, it is used in a wide range in agriculture, causing a high level of waste in the aquatic environment and food commodities, causing severe harm to humans. Thus, to ensure food safety, developing a simple and effective method for identifying pesticides in environmental and food samples is extremely important (Brutti et al. 2010).

Carboxylic acid pesticides were used extensively in agriculture to improve the productivity of agricultural products such as 2-(4-chloro-2-methylphenoxy) acetic acid (MCPA), 2-(2,4-dichlorophenoxy) propanoic acid, 2,4-dichlorophenoxyacetic acid (2,4-D), imidacloprid, (2,4-DP), 2-(2,4,5-trichloro phenoxy) acetic acid (2,4,5-T), 4-chlorophenoxyacetic acid (4-CPA), and cyhalothrin. Some of these acidic pesticides are endocrine disrupters and cause carcinogenic and teratogenic diseases. They can easily reach the surface water or via leakage or natural drainage due to their good solubility and high polarity. The superior pollutant level of

chlorophenoxy acid herbicides in water is in the range of $10\text{--}70 \text{ ng mL}^{-1}$. The maximum efficiency and selectivity of carboxylic acid pesticides is a big challenge due to their strong water solubility.

Ji et al. reported the amino covalent organic framework ($\text{NH}_2\text{@COF}$) which is synthesized by the thiol-ene click reaction of the vinyl covalent organic framework (COF) with 4-aminobenzenethiol (Ji et al. 2019b). $\text{NH}_2\text{@COF}$ is distinguished by an excellent extraction ability for carboxylic acid pesticides with both better extraction performance than commercial adsorbents and superior selection compared with the unfunctionalized COF. $\text{NH}_2\text{@COF}$ showed a maximum adsorption capacity of $q_{\text{max}} > 10.5 \text{ mg g}^{-1}$ for six carboxylic acid pesticides (Dicamba, 2,4,5 T, 2,4 DP, 4-CPA, 2,4 D, and MCPA) while vinyl COF provides adsorption quantities with $q_{\text{max}} < 1.5 \text{ mg g}^{-1}$ lower than $\text{NH}_2\text{@COF}$ due to stronger intermolecular interactions between hydrophilic pesticides and $\text{NH}_2\text{@COF}$. Furthermore, the adsorption capacity values for cyhalothrin 379 (1.27 mg g^{-1}) tsumacide (1.48 mg g^{-1}), and imidacloprid (1.32 mg g^{-1}) were reduced by the hydrophilicity of $\text{NH}_2\text{@COF}$. Weak interactions lead to a significantly lower adsorption capacity of both vinyl COF and $\text{NH}_2\text{@COF}$ for gentamycin ($q_{\text{max}} < 1.0 \text{ mg g}^{-1}$). $\text{NH}_2\text{@COF}$ captures six pesticides that are kinetically efficient and equilibrium adsorption capacity reaches within 25 min Table 2. Besides, the pseudo-second-order model can manifest that the removal of six carboxylic acid pesticides mostly depends on chemical adsorption (Ji et al. 2019b).

Benzoylureas pesticides (diflubenzuron), hexaflumuron, chlorfluazuron, triflumuron, and flufenoxuron are acted as insect growth regulators (Stuart & Lapworth 2013). Song et al. reported DAAQ-TFP COF used to extract five different classes of compounds, including phenyl urea herbicides, phthalic acid esters, endocrine disruptor chemicals, chlorophenols, and benzoylurea insecticides (Bus). It showed good thermochemical stability, high porosity, large surface area, and abundant O and N groups make it have great potential as a platform for Bus. It was used as an adsorbent to extract benzoylurea insecticides from the water with high adsorption capacity at low detection limits. Owing to its high π -conjugated system, DAAQ-TFP can form a strong π -interaction with some aromatic compounds. Among different adsorbents, DAAQ-TFP showed the highest extraction recovery for benzoylurea insecticides. So, the DAAQ-TFP was used as a promising platform to extract organic compounds like Bus (Song et al. 2018).

Organic dyes

One of the most common industrial water contaminants is pigments, which have presented serious environmental and human health risks (Hasan & Jhung 2015, Nguyen & Juang 2013). From the global dye production (around 800 000 tons

/year), approximately 10–15% enter the ecosystems directly as effluent or because of losses that happened through techniques (Hassaan et al. 2017). The removal of dyes from water is further categorized depending on their charge of molecular (neutral, anionic, and cationic) at neutral pH, usually present in wastewater.

Cationic dyes

Cationic dyes can be separated into positively charged ions in water such as rhodamine B, crystal violet, N, N-dimethyl-p-phenylenediamine dihydrochloride, brilliant green, and methylene blue. Triphenylmethyl dyes, one of the principal categories of pigments, are widely used in industries (e.g., pharmacology, plastic, rubber, textile, and printing) (Chaudhry et al. 2014; Liu et al. 2019). These dyes are usually poisonous and carcinogenic and may pose a serious threat to organisms in water and humans (Vyavahare et al. 2018; Ye et al. 2019). They are very soluble in water and extremely resistant to degradation in sunlight and heat, so removing dyes from water is critically significant for ecosystem protection and the health of humans.

To date, very few techniques have been used for the elimination of triphenylmethyl dyes, such as membrane filtration for adsorption (Amirilargani et al. 2019), chemical oxidation (Sirés et al. 2008), photodegradation (Wang et al. 2014a), AOPs, and biological technologies (Chen & Ting 2015). Adsorption usually requires more time to attain equilibrium to absorb dye and adsorption (Rajabi et al. 2017; Yusuf et al. 2015), resulting in a long-time capture process. Hence, exploring new sorbents with fast kinetics of adsorption and great adsorption quantities is of great importance and challenge for the adsorption and removal of organic dyes. Li et al. reported (COF-TzDBd) for very fast adsorption and efficient elimination of triphenylmethane dyes with mesoporous pores, good crystallinity, and high chemical stability. The maximum adsorption capacities of crystal violet and brilliant green on TzDBd were 307 and 276 mg g⁻¹ respectively. The equilibrium time for adsorption crystal violet and brilliant green was obtained in 15 min (Li et al. 2019a).

Wang et al. reported covalent triazine framework (CTF) used as an adsorbent for adsorption organic dyes due to its microporous structure, high surface area 2071 m² g⁻¹. It demonstrated a higher adsorption capacity of rhodamine B (1.01 mmol/g) than classical platforms such as AC with q_{max} (0.36 mmol/g). An increasing temperature was desired for the adsorption of rhodamine B onto CTF. As the temperature increased, the capture of rhodamine B by CTF increased. the maximum uptake (0.51 mmol/g) at 45 °C with an equilibrium time of 25 min. Kinetics and mechanism investigation showed that the adsorption of rhodamine B onto CTF is subjected to the Langmuir isothermal adsorption model

and follows a pseudo-second-order adsorption equation, with equilibrium time 55 min Table 3 (Wang et al. 2014b).

CuP-DMNDA-COF/Fe was synthesized by modifying imine-linked porphyrin COF with FeCl₃ in acetone. The removal efficiency of rhodamine B by CuP-DMNDA-COF/Fe was affected by the coordinate interactions between Fe (III) ions in the COF and the carboxy group of rhodamine B. Thermodynamics was used to study the adsorption performance, and the results demonstrated a spontaneous and endothermic process (Hou et al. 2017). TPT-azine-COF and TPT-TAPB-COF are also showed high adsorption capacity of rhodamine B with q_{max} = 725 and 970 mg/g respectively. The high removal efficiency ascribed to the higher surface areas (957 m²/g for TPT-TAPB-COF and 1,020 m²/g for TPT-azine-COF). Both COFs exhibited high selectivity and regeneration ability (Li et al. 2018).

Huo et al. introduce TPT-DMBD-COF with high porosity, a large specific surface area (279.5 m²·g⁻¹) for adsorption methylene blue. At the low pH of the methylene blue, the solution was acidic which competed for a large amount of H⁺ and MEB (positively charged). So, the adsorption efficiency of methylene blue was relatively low under acidic conditions. When the methylene blue solution was basic (pH is 10), the maximum adsorption was 12.31 mg·g⁻¹ (Huo 2019). Zhu et al. introduce TS-COF-2 as an efficient adsorbent for removal methylene blue, and rhodamine B. COF exhibits high adsorption of the.

Zhang et al. presented the EB-COF: Br membrane as excellent selective sieving carried out for different dye molecules/ions, which ascribed to their positively charged sites on the walls in addition to small pores. Cationic EB-COF: Br nanosheets 2D was reported as adsorbent for removal of cationic dye N, N-dimethyl-p-phenylenediamine dihydrochloride, methyl blue, and rhodamine B. The rejection values of cationic dyes N, N-dimethyl-p-phenylenediamine dihydrochloride, methyl blue, and rhodamine B are 84.9%, 87.2%, and 91.2%, respectively. Cationic dye molecules N, N-dimethyl-p-phenylenediamine dihydrochloride can diffuse into the channels slowly because of the small size of N, N-dimethyl-p-phenylenediamine dihydrochloride dye. Because of the repulsive force between the positively charged pore and the cationic dye, the cationic dye is unable to enter the channels, and these dyes will pass through the membrane (Zhang et al. 2018b).

Anionic dyes

Anionic dyes can be separated into negatively charged ions in water such as dye potassium permanganate (PP), brilliant red X-3B, scarlet 4BS, alizarin red (AR), methyl orange (MO), methyl blue MB, direct fast brown M (DFBM), acid green 25 (AG), fluorescein sodium salt (FSs), acid red 27 (AR-27) and indigo carmine (IC). As discussed before, CTF

is used as a platform for adsorption cationic dye RhB and is also used for adsorption anionic dye brilliant red X-3B and scarlet 4BS with uptake reaches 0.43 and 0.18 mmol/g for X-3B and 4BS, respectively. For anionic dyes, the interaction between the adsorbent of the free electrons of the dye molecule and the surface basic sites is the main adsorption mechanism (Wang et al. 2014b).

BTT-TAPT-COF showed excellent adsorption capacity removal of indigo carmine dye with 547.33 mg g^{-1} . It was found that the Langmuir model showed better linearity than the Freundlich model due to better clarify of indigo carmine adsorption onto BTT-TAPT-COF and formation of monolayer adsorption of IC. The recycling adsorption was performed of BTT-TAPT-COF toward indigo carmine dye after five cycles (Pan et al. 2020). Yu et al. introduced 2D (PC-COF) imine linkage with high stability in water and high adsorption quantities ($> 97\%$) for removal of anionic organic dye contaminants (methyl orange, monoanionic, acid green 25, dianionic, direct fast brown M, dianionic, indigo carmine, dianionic, and acid red, trianionic) at low concentration ($3.2 \times 10^{-5} \text{ M}$) from water. The equilibrium time of methyl orange was reached at 30 min (Yu et al. 2016).

TS-COF-2 was reported for adsorption cationic dye methyl blue, and rhodamine B, it is also used for adsorption anionic dye (CR) with $q_{\text{max}} = 319 \text{ mg g}^{-1}$. The best adsorption wavelengths of CR were reported 500 nm, the Langmuir and Freundlich isotherm models were used to fit the adsorption data which showed a good linear relationship at equilibrium. The maximum adsorption capacity of TS-COF-1 was 319 and 46.02 mg g^{-1} by the Langmuir and Freundlich model respectively which higher than that of polyvinyl alcohol/activated carbon, polyvinyl alcohol hydrogel, and melamine–formaldehyde polymer.

Cationic EB-COF: Br nanosheets 2D was reported as a sieving membrane for removal of anionic dye fluorescein sodium salt, methyl orange, and potassium permanganate. the membrane can refuse anionic dyes potassium permanganate, fluorescein sodium salt, and methyl orange up to 98.1%, 99.2%, and 99.6%, respectively. The regeneration of COF was performed by immersing the membrane with an aqueous NaBr solution and the rejection efficiency for methyl orange is above 99.1% even after six cycles (Zhang et al. 2018b).

Neutral dyes

Neutral dyes are salt formed by the interaction of an acid dye and a basic dye. Using COFs in the capture of neutral dyes is very limited compared to the cationic and/or anionic dyes and is directly related to adsorption. Generally, the COF adsorption quantity of neutral dyes is less than that of cationic and/or anionic dyes (Table 3). Taking into account the existence of negative or positive structures in the framework,

higher adsorption of anionic and cationic dyes is referred to as the formation of π - π interactions and electrostatic interactions between the matrix and dye. Cationic EB-COF: Br nanosheets 2D was reported as a sieving membrane not only for anionic and cationic dyes but also for neural dye. The Nile red, calcein, and p-nitroaniline were selected for rejection on EB-COF: Br membrane, the selectivity of sieving for dye molecules depended on their different sizes and charges. UV–vis absorption spectra of neutral dye solutions before and after sieving by the EB-COF: Br approved the rejection of Nile red, calcein, and p-nitroaniline on EB-COF: Br membrane. The rejection efficiency values of p-nitroaniline, Nile red, and calcein were 15.7%, 22.3%, and 74.4%, respectively. For neutral dye molecules, the electrostatic interaction is very weak between the EB-COF: Br and dye. Therefore, the rejection efficiency is mainly attributed to the effect of molecular size sieving. The order of molecular size of neutral dye is p-nitroaniline $<$ Nile red $<$ calcein which can pass through the pore channels of the EB-COF: Br membrane.

Industrial organic water contaminations

In developed societies, rapid industrialization is associated with the production of large quantities of factory waste to meet the increasing demand for consumer products (Dhaka et al. 2019, Rojas & Horcajada 2020). Many industrial organic/inorganic contaminants have a significant impact on water pollution. The wide use of aromatic compounds in the industry led to potential environmental risks due to high toxicity rates, high oxygen demand, carcinogenicity, and low biodegradability. Therefore, eliminating these contaminants from polluted water is very significant for water treatment (Erogul et al. 2015; Liu et al. 2014). Some traditional porous synthetic organic materials such as polymeric resins have already been extensively used as platforms for organic water pollutants and environmental remediation recently (Buchmeiser & Catalysis 2003). COFs have also been suggested as an excellent platform for the removal of this kind of pollutants.

Pollution of our environments with nitrobenzene derivatives (NBD) has become a global concern with toxins. The extensive use of NBD in industries has raised the level of NBD in wastewater to 100 ppm. Its high solubility and poisonousness make it an urgent contaminant for various environmental organizations. Hence, the search for effective platforms to recover the NBD from water is very important. Naphthols are extensively used as an intermediate material in diverse industrial development to manufacture products related to modern societies. The effect of toxicity of naphthol on both organisms with wide use and high mobility makes this, besides pollutants pose a dangerous risk to the environment's sustainability. Liu et al. showed the adsorption efficiency of CTF for aromatic compounds

such as phenol (PHOL), benzene (BEN), benzenesulfonate (BS), aniline (AN), 1,3-dinitrobenzene (DNB), nitrobenzene (NB), 4-ethyl-2,6-dinitrophenol (MDNP), 1,3,5-trinitrobenzene (TNB), naphthalene (NAPH), 1-naphthalenamine (1-NALA), 2-naphthol (2-NAOL), 2-naphthalenesulfonate (2-NS). CTF exhibited high selectivity toward NAPH, 2-NAOL, 2-NS, 1-NALA, DNB, MDNP, BEN, BS, and TNB compared to a polymeric adsorbent amberlite XAD-4 resin Table 4. By comparing the adsorption and uptake kinetics of nitrobenzene between CTF and XAD-4, the equilibrium time reached within 100 min on CTF, but within 600 min on XAD-4 (Liu et al. 2012).

Ji et al. introduced DhaTab-PBA for adsorption hydroquinone, resorcinol, toluene, phenol, catechol, aniline, and chlorobenzene with good thermal and chemical stability. DhaTab-PBA showed selectivity toward catechol with q_{\max} of 160 mg g^{-1} (Table 4). The large adsorption capacity for removal catechol was due to π - π interaction. The adsorption capacity of catechol on DhaTab-PBA increased in the pH range 3–7 and remained almost constant from pH 7 to pH 10. The equilibrium time for desorption catechol on DhaTab-PBA was reached within 40 min, which indicated the fast catechol adsorption. Regenerated COF was performed by phosphate buffer solution (PBS), 10 mM, with an even after five adsorption-adsorption cycles (Ji et al. 2019a).

Bisphenol A is extensively used to manufacture epoxy resins and polycarbonate plastics. It is one of the most chemicals that is produced globally. The presence of bisphenol A in the water has devastating effects on the endocrine system; hence the main focus is on the issue of the environment (Mon et al. 2018). Wei et al. presented $\text{Fe}_3\text{O}_4@\text{TpND}$ for removal bisphenol A with a high $q_{\max} = 114.97 \text{ mg g}^{-1}$ at pH 6. The equilibrium of adsorption attained 10 min and was maintained over the entire range of contact time. The kinetic process of bisphenol A adsorption on $\text{Fe}_3\text{O}_4@\text{TpND}$ was described to introduce the pseudo-first-order and pseudo-second-order models. Five sorption-regeneration cycles were carried out to test the adsorption capability. After five cycles, the capture efficiency was kept at about 96.2%, indicating the high recyclability of $\text{Fe}_3\text{O}_4@\text{TpND}$ (Wei et al. 2020b).

Fermentation of carbohydrate substrates produces lactic acid, but isolating it from the broth generates equivalent amounts of residual salt precipitated. While the demand for lactic acid is extremely growing; this separation problem is the basic narrow reducing the generation process's further upscaling. Lohse et al. introduced three COFs, $\text{TpBD}(\text{NHCOCH}_3)_2$, $\text{TpBD}(\text{NH}_2)_2$, $\text{TpBD}(\text{NO}_2)_2$ for adsorption lactic acid. COFs, $\text{TpBD}(\text{NHCOCH}_3)_2$ was synthesized via acetylation of $\text{TpBD}(\text{NH}_2)_2$ which was formed by reduction of $\text{TpBD}(\text{NO}_2)_2$. Three COFs was used as adsorbent for the adsorption of lactic acid. The maximum adsorption capacity of $\text{TpBD}(\text{NHCOCH}_3)_2$, $\text{TpBD}(\text{NH}_2)_2$ and

$\text{TpBD}(\text{NO}_2)_2$ for lactic acid $q_{\max} = 4.0$, 6.6 and 2.4 mg/g receptivity at natural pH. A small polar.

molecule lactic acid adsorbed by π - π -interactions of COF stacks for three COFs as well as H-bond donor and acceptor atoms, of $\text{TpBD}(\text{NHCOCH}_3)_2$ and $\text{TpBD}(\text{NH}_2)_2$. Different shapes of isotherm were observed for the three COFs, $\text{TpBD}(\text{NH}_2)_2$ and $\text{TpBD}(\text{NHCOCH}_3)_2$ showed type I isotherms with uptakes of up to 6.6 and 4.0 wt%, respectively, but the isotherm of $\text{TpBD}(\text{NO}_2)_2$ was linear with a highest measured uptake at 2.5 wt%). These results showed that lactic acid adsorption could be adsorbed by the chemical pore environment (Lohse et al. 2016).

The contamination of ground and surface water by polyfluorinated alkyl substances affects all humans worldwide. Polyfluorinated alkyl substances, like perfluorooctanoic acid, perfluorooctane sulfonate, and ammonium perfluoro-2-propoxypropionate. Polyfluorinated alkyl substances are used in the generation of water, fluoropolymers, and stain repellents and as ingredients of aqueous film-forming foams used to inhibit fires. Concerns about environmental persistence, bioaccumulation, and health effects of perfluorooctanoic acid allowed it to be phased out in the United States. However, it has been altered by other polyfluorinated alkyl substances, such as ammonium perfluoro-2-propoxypropionate, which are also dangerous contaminants. Ammonium perfluoro-2-propoxypropionate was originated in the Cape Fear River in North Carolina, and its elimination by traditional and progressive treatment technologies was negligible. Dichtel et al. presented imine-linked two-dimensional (2D) COFs (having primary amines) adsorb ammonium perfluoro-2-propoxypropionate rapidly at environmental concentration with high surface area $\geq 1000 \text{ m}^2 \text{ g}^{-1}$ and crystallinity materials. The $X\%[\text{NH}_2]$ -COFs exhibit high affinity for adsorbing ammonium perfluoro-2-propoxypropionate and other polyfluorinated alkyl substances. The removal efficiency values of COF with 100% $[\text{NH}_2]$ -COF and 20% $[\text{NH}_2]$ -COF were 56 and 97% respectively. The highest adsorption capacity of 20% $[\text{NH}_2]$ -COF due to having the highest affinity to ammonium perfluoro-2-propoxypropionate. Whereas at lower amine loadings, GenX uptake was slightly decreased for 10% $[\text{NH}_2]$ -COF and 1% $[\text{NH}_2]$ -COF with a removal efficiency of 94% 73%. The mechanism of interaction of GenX with the amine-functionalized COFs was proposed to arise from favorable interactions of the polar amino groups with the anionic headgroup of ammonium perfluoro-2-propoxypropionate. The $X\%[\text{NH}_2]$ -COFs showed rapid removal for adsorbing GenX and other polyfluorinated alkyl substances and reached equilibrium time at 30 min (Ji et al. 2018).

Overall, organic pollutants are classified into pharmaceuticals, pesticides, dyes, and industrial by-products. The adsorption performances by COFs are summarized and tabulated in Tables 1, 2, 3, to 4. These compounds have polluted the water of the environment around the world, mainly due

to runoff from firefighting foams, effluents, and a variety of industrial processes. However, COF-based materials are showed high removal efficiency of these pollutants, the practical use of COFs as adsorbents was limited. Reusability and long-term stability of COFs will also need to be achieved to enable most real applications.

Adsorption mechanism of COFs

Understanding the adsorption mechanism is very important because the interactions between the adsorbate – adsorbent are significant for designing future materials. Generally, adsorption performances are affected by two factors: (1) the interaction between organic contaminants and COFs such as the electrostatic attraction, hydrogen bond, hydrophobic interaction, dispersive interaction, and π - π .

Electrostatic interaction

Electrostatic interaction plays an important role in the adsorption process. The interaction occurred between the charge on the surface area of COFs and the opposite charge of adsorbate (organic pollutants). Electrostatic interaction is mainly affected by the solution of pH which influences (1) proton/deprotonation of the functional groups, (2) changing the distribution of pollutants species, and (3) changing the charge on the surface of COFs. For example, TPB-DMTP-COF was used for adsorption sulfamethazine, TPB-DMTP-COF was synthesized by condensation of 2,5-dimethoxyterephthalaldehyde and 1,3,5-tri-(4-aminophenyl) benzene. It was exhibited a large surface area ($2115 \text{ m}^2/\text{g}$), and high crystallinity. The imine group ($\text{C}=\text{N}$), and OR play an important role in the removal mechanism. Sulfamethazine was trapped in the pore size of COF with its π -rings facing the walls of COFs. The maximum adsorption capacity of sulfamethazine was at $\text{pH}=6$ while the adsorption performance was lower in acidic or alkaline conditions due to the electrostatic repulsive forces increased significantly (Zhuang et al. 2020b). Moreover, TzDBd showed ultrafast adsorption of triphenylmethane dyes (brilliant green and crystal violet). It was synthesized by direct condensation of 1,3,5-tris(4-formyl-phenyl) triazine (Tz) and 4,4'-diamino-[1,1'-biphenyl]-2,2'-dicarboxylic acid (DBd). It showed good crystallinity, mesoporous pores, and high chemical stability. The adsorption of brilliant green and crystal violet by TzDBd COF increased as the pH was increased from 3 to 5. At $\text{pH}=3$, the electrostatic repulsion between cationic dyes (BG and CV) and positively charged of TzDBd COF resulted in inappropriate adsorption of brilliant green and crystal violet on TzDBd. (Li et al. 2019a)

BTT-TAPT-COF showed high crystallinity, large surface area, and thermal stability. Due to the porous feature, the large π -conjugated network structure, and the existence of

electron-rich heteroatoms. It exhibited excellent adsorptive performance for the removal of indigo carmine with an adsorption capacity of 547.33 mg g^{-1} . The removal mechanism of indigo carmine onto BTT-TAPT-COF has been suggested through electrostatic reaction. At low $\text{pH}=2$, N and S functionalized BTT-TAPT-COF were protonated to yield a large amount of positively charged sites that interact with negatively charged anionic indigo carmine dye. Therefore, the removal efficiency of indigo carmine was improved. However, at high $\text{pH}=10$, the protonated process was hindered due to the low H^+ concentration (Table 5). As a result, the adsorption capacity decreased, especially at $\text{pH}=10$. Also, the amino-modified covalent organic framework ($\text{NH}_2@$ COF) showed an excellent extraction ability for carboxylic acid pesticides. The introduction of amino groups can interact with the anionic headgroup of carboxylic acid pesticides. Moreover, the ample hydrophilic surface area can boost absorption in the water media. Electrostatic attraction between the carboxyl group of pesticides and the amino group of $\text{NH}_2@$ COF has been suggested to be the main mechanism for the uptake. As well, cationic EB-COF: Br nanosheet was synthesized by a facile bottom-up interfacial crystallization. It showed much higher solvent permeability due to its high porosity. The main mechanism of cationic EB-COF: Br nanosheets 2D for the removal of fluorescein Sodium salt, methyl orange, and potassium permanganate depended on the strong electrostatic interaction between anionic dyes and the positively charged pore walls of the membrane. Moreover, the nanoscale size of channels limits the adsorption of the dye.

TPT-DMBD-COF was synthesized by the condensation of the O-linked, flexible, triazine-based aldehyde TPTCHO and the rigid diamine DMBD. It was exhibited permanent porosity, a high specific surface area ($279.5 \text{ m}^2\cdot\text{g}^{-1}$), and was chemically and thermally stable. It can adsorb methylene blue in basic or neutral conditions because the functional groups on the surface of COF are electronegative under basic or neutral conditions which indicate an electrostatic attraction between the positive charge of the amine group ($-\text{N}^+=$) of methylene blue dye molecule and the surface negative charge of TPT-DMBD-COF (Huo 2019).

Molecular size effect

The design of candidates with suitable pores size is the critical challenge in environmental remediation for eliminating organic contaminants. Moreover, the size of adsorbate has also participated in the adsorption. For instance, benzimidazole-COF was synthesized through Schiff base condensation to trigger their ionization response both under acid and basic conditions. It was used for the removal of four dyes (methyl orange, methyl blue, acid magenta, and crystal violet). Methyl orange and methyl

blue were adsorbed because of their smaller size than acid magenta and crystal violet. Therefore, both dyes showed higher adsorption capacity (256 mg/g) for methyl orange in acidic conditions and (185 mg/g) for methyl blue in basic conditions (Xu et al. 2020).

CH/ π -interaction and π - π interaction

CH/ π - interaction with some aromatic compounds (non-covalent bond) where the region of positive charge interacts with a negative charge (the electron-rich π system can interact with cation, neutral, anion, another molecule, and even another π system) (Mori & Inoue 2005). DAAQ-TFP possesses a large surface area, high porosity, and good thermochemical stability. It poses a high π -conjugated system that forms a strong π -interaction with some aromatic compounds (Table 5). It was employed as an adsorbent to extract benzoylurea insecticides (BUs) from environmental water, juice, fruit, and vegetable samples. The abundance of O atoms and N–H groups makes it of great potential as an adsorbent for some compounds. (Song et al. 2018). Moreover, TS-COF-2 is mesoporous triazine-functionalized polyimide COF. The adsorption of methylene blue by TS-COF-2 is explained by both the size of the organic dye molecules and the intrinsic pore size. The diversity of COF based-materials and the understanding of organic dyes' encapsulation on COFs possess great promise for developing new COF candidates for the efficient capture of organic pollutants from the aquatic environment (Zhu et al. 2017).

Hydrogen bond

The hydrogen bond is participated in the extract of benzoylurea insecticides by DAAQ-TFP. DAAQ-TFP has abundant O atoms and N–H groups, which make hydrogen bonding stronger (Song et al. 2018). Also, the adsorption mechanism of diclofenac by COF-SO₃H through π - π interactions and hydrogen bonds formation, in which the π -electrons number of the adsorbate and adsorbent was constant. At pH 6–10, the amino (–NH) group is stable on diclofenac, SO₃– on COF ionized and the oxygen atom in the sulfonic acid group can form an intermolecular hydrogen bond with the hydrogen of the amino group of diclofenac. Moreover, Fe₃O₄@COF(TpBD)@Au-MPS showed a high affinity to fluoroquinolones owing to the ionic interactions and hydrogen bond between the magnetic surface of COF and fluoroquinolones. Furthermore, hydrogen bonding dominated the removal mechanism for bisphenol A by Fe₃O₄@TpND (Wei et al. 2020b) (Table 5).

Hydrophobic interaction and others

One interesting approach for the adsorption of organic pollutants from an aqueous solution is hydrophobic COFs. PC-COF was successfully synthesized by a facile solution-processed condensation polymerization with the raw materials 1,3,5-tris(4 aminophenyl) benzene and 1,1-bis(4-formylphenyl)-4,4'-bipyridinium dichloride. PC-COF is polycationic two-dimensional (2D), that the 2D layer structures stack into 3D porous frameworks and the adjacent BIPY dications stack in an eclipsed pattern, with chloride counterions being sandwiched in between the layers. It showed high adsorption efficiency (97%) for removal of acid green 25, methyl orange, indigo carmine, direct fast brown M, acid red 27 over water. Hydrophobic and electrostatic attraction between the anionic groups of the dyes and the bipyridinium dications of the COF was suggested to be the main mechanism for the uptake. While the exchange of hard base Cl[–] with the dye anion as soft base plays an important role due to the formation of two hard acid-hard base and soft acid soft base pairs. (Table 5) (Yu et al. 2016).

Wang et al. reported a solid-phase microextraction approach to remove seven phenols (phenol, 4-bromophenol, 4-chlorophenol, 2,3-dichlorophenol, 2,4-dichlorophenol, 2,3,6-trichlorophenol, and 3,4-dichlorophenol). The high removal of these dyes has indicated that π - π stacking interactions, π conjugation of aromatic groups, and hydrophobic interaction have dominated the capture reactions between SNW-1-coated fiber and contaminants (Wang et al. 2016).

The removal mechanism of rhodamine B onto CTF can be concluded such that (1) The basic sites for the adsorption of dyes are rich in carbon and nitrogen. (2) The electrostatic interaction is more significant than the interaction between the primary surface site and a free electron. (3) Dispersion is significant for dyes to enter the pores. Also, π - π interaction in mesoporous pores and electrostatic interaction contributed to the adsorption. TzDBd gave faster kinetics for the adsorption of cationic dyes as compared to other platforms involving commercial activated carbon. It was found that ethanol and HCl (10 mM) were not satisfied with the desorption efficiency to reusability, so an ethanol solution with (0.1%) hydrochloric acid was used; the efficiency was increased to 95% desorption. The results showed that electrostatic interaction and π - π interaction affected the adsorption, the HCl solution led to electrostatic repulsion between the analytes and adsorbent. Simultaneously, the organic solvent allowed triphenylmethane dyes to be more soluble, this also indicated the synergistic effects of the electrostatic and π - π interaction during the adsorption process (Table 5) (Li et al. 2019a). Moreover, the adsorption mechanisms of CTF depended on electrostatic attraction, non-hydrophobic including hydrogen bonding (amino- and hydroxyl-substituted compounds), and π - π electron-donor-acceptor interaction with the triazine

Table 5 Illustration of interaction between organic contaminants and COFs during adsorption

COF-based materials	COFs functional group types	Reaction mechanism	Capture ways	Reference
Pharmaceutical contaminations and Personal Care Products (PPCPs)				
MCOF-2	NH, C=O	MCOF-2-NH/C=O + ⁻ OOC-diclofenac Sodium → [MCOF-2-NH/C=O..... ⁻ OOC-diclofenac Sodium]	Electrostatic interaction and $\pi-\pi$ interaction	(Huang et al. 2019)
TpBD-(CF ₃) ₂	NH, C=O	TpBD-(CF ₃) ₂ -NH/C=O + HOOC-ibuprofen → [TpBD-(CF ₃) ₂ -NH/C=O.....HOOC-ibuprofen]	Electrostatic interaction	(Mellah et al. 2018)
TPB-DMTP-COF	=N-, OR	TPB-DMTP-COF=N-/OR + H ₂ N-sulfamethazine → [TPB-DMTP-COF=N-/OR.....H ₂ N-sulfamethazine]	Electrostatic interaction and C-H... π interaction	(Zhuang et al. 2020b)
β -cyclodextrin COF	NH ₂ , OH	β -cyclodextrin COF-NH ₂ /OH + OH-bisphenol A → [β -cyclodextrin COF-NH ₂ /OH.....OH-bisphenol A]	Ion exchange, $\pi-\pi$ interaction, hydrogen bonding, and hydrophobic interactions	(Wang et al. 2018b)
TAB-DVA-COF	-NH	TAB-DVA-COF-NH + HOOC-naproxen → [TAB-DVA-COF-NH.....HOOC-naproxen]	$\pi-\pi$ interaction and hydrogen bonding	(Hao et al. 2019)
COF-SO ₃ H	-NH, -SO ₃	COF-SO ₃ H/NH + HOOC-indomethacin → [COF-SO ₃ H/NH.....HOOC-indomethacin]	$\pi-\pi$ interaction and hydrogen bonding	(Hao et al. 2019)
Fe ₃ O ₄ @COF(TpBD)@Au-MPS	-C=N-, OH, SO ₃ ²⁻	Fe ₃ O ₄ @COF(TpBD)@Au-MPS - OH/SO ₃ ²⁻ + HO/HN-danofloxacin → [Fe ₃ O ₄ @COF(TpBD)@Au-MPS - OH/SO ₃ ²⁻HO/HN-danofloxacin]	Electrostatic interaction, hydrogen bonding, and $\pi-\pi$ interaction,	(Wen et al. 2020)
Magnetic TPB-DMTP-COF	=N-, OR	Magnetic TPB-DMTP-COF=N-/OR + H ₂ N-sulfamethazine → [Magnetic TPB-DMTP-COF=N-/OR.....H ₂ N-sulfamethazine]	$\pi-\pi$ interaction and C-H... π interaction	(Zhuang et al. 2020a)
NCCT	=N-, OH	NCCT=N-/OH + H ₂ N-cefotaxime → [NCCT=N-/OH.....H ₂ N-cefotaxime]	$\pi-\pi$ interaction and hydrogen bonding and electrostatic interaction	(Li et al. 2020b)
Pesticides				
NH ₂ @COF	NH ₂ , =N-, SR-	NH ₂ @COF=N-/NH + HOOC-dicamba → [NH ₂ @COF=N-/NH.....HOOC-dicamba]	Electrostatic interaction	(Ji et al. 2019b)
vinyl covalent organic framework (COF)	=N	vinyl covalent organic framework (COF)=N + HN-imidacloprid → [vinyl covalent organic framework (COF)=N.....HN-imidacloprid]	Electrostatic interaction	(Ji et al. 2019b)
DAAQ-TFP	C=O-, NH	DAAQ-TFP-C=O + ROOC-phthalic acid esters → [DAAQ-TFP-C=O.....ROOC-phthalic acid esters]	$\pi-\pi$ interaction and hydrogen bonding	(Song et al. 2018)

Table 5 (continued)

COF-based materials	COFs functional group types	Reaction mechanism	Capture ways	Reference
Electrospun COFs/polyacrylonitrile Nanofibers	= N	Electrospun COFs/polyacrylonitrile Nanofibers = N- + HNOOC- methomyl → [Electrospun COFs/polyacrylonitrile Nanofibers = N-..... HNOOC- methomyl]	Electrostatic interaction	(Li et al. 2020a)
Fe ₃ O ₄ @SiO ₂ -NH ₂ @COFs	= N	Fe ₃ O ₄ @SiO ₂ -NH ₂ @COFs = N- + HNOOC- methomyl → [Fe ₃ O ₄ @SiO ₂ -NH ₂ @COFs = N-..... HNOOC- methomyl]	Electrostatic interaction	(Li et al. 2020a)
Organic dyes				
CTF	= N-N = N-	CTF -N = N- + HOOC- rhodamine B → [CTF -N = N-/OR..... HOOC- rhodamine B]	Electrostatic and dispersive interaction	(Wang et al. 2014b)
COF-TzDBd	= N-N = N-, -C = N-, COOH	COF-TzDBd = N-/COOH + R ₂ N- crystal violet / R ₂ N brilliant green → [COF-TzDBd = N-/COOH..... R ₂ N- crystal violet / R ₂ N brilliant green]	Electrostatic and π-π interaction	(Li et al. 2019a)
TPT-DMBD-COF	-N = , O	TPB- DMTP -COF = N-/OR + H ₂ N- sulfamethazine → [TPB- DMTP -COF = N-/OR..... H ₂ N- sulfamethazine]	Electrostatic and π-π interaction	(Huo 2019)
benzodiazimidazole-COF	-C = N-, OH, NH	benzodiazimidazole-COF = N-/OH/NH + HO ₃ S/R ₂ N- methyl orange → [benzodiazimidazole-COF = N-/OH/NH..... HO ₃ S/R ₂ N- methyl orange]	Electrostatic interaction	(Xu et al. 2020)
TS-COF-2	= N-N = N-, -C = N-, OH	TS-COF-2 N = N- + R ₂ N- methylene blue → [TS-COF-2 N = N-..... R ₂ N- methylene blue]	Electrostatic interaction	(Zhu et al. 2017)
BTT-TAPT-COF	= N-N = N-, -C = N-, S	BTT-TAPT-COF N = N- / OH + ⁻ O ₄ S / HN- indigo carmine → [BTT-TAPT-COF N = N- / OH..... ⁻ O ₄ S / HN- indigo carmine]	π-π interaction and electrostatic attraction	(Pan et al. 2020)
PC-COF	-N ⁺	PC-COF -N ⁺ + HO ₃ S/R ₂ N- methyl orange → [PC-COF -N ⁺ HO ₃ S/R ₂ N- methyl orange]	Electrostatic attraction and hydrophobic interaction	(Yu et al. 2016)
Cationic EB-COF:Br	-N = , O	Cationic EB-COF:Br = N- / OR + R ₂ N- Nile red → [Cationic EB-COF:Br = N- / OR..... R ₂ N- Nile red]	Electrostatic and dispersive interaction	(Zhang et al. 2018b)
Industrial organic contaminants				
MCOF-2	= N-N = N-	MCOF-2- N = N + OOC- diclofenac Sodium → [MCOF-2-NH/ C = O..... ⁻ OOC- diclofenac Sodium]	Electrostatic interaction and π-π interaction	(Liu et al. 2012)
DhaTab-PBA	-C = N-	DhaTab-PBA-C = N + HO-catechol → [DhaTab-PBA-C = N → HO-catechol]	π-π interactions	(Ji et al. 2019a)

Table 5 (continued)

COF-based materials	COFs functional group types	Reaction mechanism	Capture ways	Reference
$\text{Fe}_3\text{O}_4@(\text{COF}(\text{TpBD})@(\text{Au-MPS}))$	-C=N-, OH, SO_3^-	$\text{Fe}_3\text{O}_4@(\text{COF}(\text{TpBD})@(\text{Au-MPS})-\text{SO}_3^-/\text{OH} + \text{HOOC- enrofloxacin} \rightarrow [\text{Fe}_3\text{O}_4@(\text{COF}(\text{TpBD})@(\text{Au-MPS})-\text{SO}_3^-/\text{OH}, \dots, \dots, \text{HOOC- enrofloxacin})]$	$\pi-\pi$ interaction, electrostatic interaction interaction and hydrogen bonding	(Wen et al. 2020)
$\text{Fe}_3\text{O}_4@(\text{TpND})$	-C=N-, OH,	$\text{Fe}_3\text{O}_4@(\text{TpND}-\text{OH} + \text{OH- bisphenol A} \rightarrow [\text{Fe}_3\text{O}_4@(\text{TpND}-\text{OH}, \dots, \dots, \text{OH- bisphenol A})]$	Hydrogen bonding	(Wei et al. 2020b)
$\text{TpBD}(\text{NHOC}_2\text{H}_5)_2$	-C=O, -NH	$\text{TpBD}(\text{NHOC}_2\text{H}_5)_2-\text{C}=\text{O} / \text{NH} + \text{HOOC lactic acid} \rightarrow [\text{TpBD}(\text{NHOC}_2\text{H}_5)_2-\text{C}=\text{O} / \text{NH}, \dots, \dots, \text{HOOC lactic acid}]$	$\pi-\pi$ interaction and hydrogen bonding	(Lohse et al. 2016)
100% $[\text{N}_3]-\text{COF}$	-NH	100% $[\text{N}_3]-\text{COF}-\text{NH} + {}^+\text{H}_4\text{N}$ perfluoro-2 propoxypropionate $\rightarrow [100\%[\text{N}_3]-\text{COF}-\text{NH} \rightarrow {}^+\text{H}_4\text{N}$ perfluoro-2 propoxypropionate]	$\pi-\pi$ interaction	(Lohse et al. 2016)
75% $[\text{N}_3]-\text{COF}$	-NH	75% $[\text{N}_3]-\text{COF}-\text{NH} + {}^+\text{H}_4\text{N}$ perfluoro-2 propoxypropionate $\rightarrow 75\%[\text{N}_3]-\text{COF}-\text{NH} \rightarrow {}^+\text{H}_4\text{N}$ perfluoro-2 propoxypropionate]	$\pi-\pi$ interaction and Hydrogen bonding	(Lohse et al. 2016)
50% $[\text{N}_3]-\text{COF}$	-NH	50% $[\text{N}_3]-\text{COF}-\text{NH} + {}^+\text{H}_4\text{N}$ perfluoro-2 propoxypropionate $\rightarrow [50\%[\text{N}_3]-\text{COF}-\text{NH} \rightarrow {}^+\text{H}_4\text{N}$ perfluoro-2 propoxypropionate]	Electrostatic interaction	(Ji et al. 2018)
28% $[\text{N}_3]-\text{COF}$	-NH	28% $[\text{N}_3]-\text{COF} + {}^+\text{H}_4\text{N}$ perfluoro-2 propoxypropionate $\rightarrow [28\%[\text{N}_3]-\text{COF} \rightarrow {}^+\text{H}_4\text{N}$ perfluoro-2 propoxypropionate]	Electrostatic interaction	(Ji et al. 2018)
20% $[\text{N}_3]-\text{COF}$	-NH	20% $[\text{N}_3]-\text{COF} + {}^+\text{H}_4\text{N}$ perfluoro-2 propoxypropionate $\rightarrow [20\%[\text{N}_3]-\text{COF} \rightarrow {}^+\text{H}_4\text{N}$ perfluoro-2 propoxypropionate]	Electrostatic interaction	(Ji et al. 2018)

structure of CTF (Liu et al. 2012). Moreover, TPT-DMBD-COF contains a large number of aromatic rings that undergo $\pi-\pi$ stacking with the methylene blue molecules during adsorption (Table 5).

Above all, the adsorption processes are mostly ascribed to electrostatic attraction, H-bonding, hydrophobic interaction, and some of the mechanisms are attributed to functional group selectivity and molecular sieving. The molecular size of the adsorbate and the pre-designed pore size of the adsorbents are very important in the adsorption process. Moreover, the introduction of heteroatoms (S, O, and N) such as amino, amide, carboxyl, hydroxyl, and thiol assist the bond formation between organic contaminants and COFs which remarkably enhance the elimination efficiencies and adsorption capacities of pollutants.

Interaction mechanism analysis

Spectroscopic techniques

Various techniques have been used to confirm the interaction mechanism such as Fourier transform infrared (FTIR) spectroscopy and X-ray photoelectron spectroscopy (XPS) (Hu et al. 2020a; Wang et al. 2019). For example, after ibuprofen adsorption, the FTIR spectrum of TpBD-(CF₃)₂ showed the appearance of 1720 cm⁻¹ which referred to the carbonyl group of the ibuprofen moiety. The slight blueshift of free ibuprofen from 1705 cm⁻¹ could be revealed a change in H-bonding under environmental adsorption. Moreover, the FTIR spectrum of NCCT-COF after the adsorption of cefotaxime (CTX) and tetracycline was found in the range of 1300–400 cm⁻¹ which agrees with the fingerprint spectrum of each antibiotic (Li et al. 2020b; Liu et al. 2021). The spectra of NCCT showed that the Fe—O and —OH peaks of NCCT were found at 575 cm⁻¹ and 3436 cm⁻¹, respectively. After adsorption of CTX and TC, the —OH peaks shifted to 3434 cm⁻¹ and 3428 cm⁻¹, respectively. For NCCT-TC adsorption, the shifting might be referred to the —OH cation exchanged with deprotonated TC molecules adsorption. Whereas NCCT-CTX adsorption, the shifting might be ascribed to the —OH the formation of intramolecular hydrogen bonding. the Fe—O of NCCT-TC shifted to 566 cm⁻¹ indicating the surface complexation of iron atoms with the species of TC while the shifting of C=C peaks from 1582 to 1599 and 1597 cm⁻¹, respectively, might be due to the $\pi-\pi$ interaction between antibiotics and NCCT (Li et al. 2020b).

XPS spectra of N 1 s of NCCT could be deconvoluted into three peaks, such as —N=, —NH, and N⁺ positive nitrogen located at 398.8 eV, 399.5 eV, and 4.2% respectively. After CTX adsorption, The peak area of —N⁺ increased rapidly from 4.2% to 47.8% and the —NH

decreased dramatically from 59.7% to 17.0%, which might be referred to the strong interaction between the amino groups of NCCT and CTX species. For TC adsorption, the peak area of Fe—O was significantly increased, indicating that the uptake of the TC on NCCT was likely attributed to the surface complexity of Fe / Ni with oxygenic groups of TC like the C1–C3 and C10–C12 portion. On the other hand, the —OH peak area of NCCT-TC decreased dramatically compared to that of NCCT. Therefore, the adsorption of TC on NCCT might be significantly enhanced by the cation exchange between the C4 amino group of TC and the hydroxyl of NCCT (Li et al. 2020b).

Wei et al. reported the elimination of (bisphenol A by Fe₃O₄@TpND. XPS spectra showed the high-resolution O 1 s for three O 1 s peaks located at 530.7 eV, 532.3 eV, and 533.8 eV, which can be referred to as the O—H, C=O, and physically adsorbed water on the metal oxide surface, respectively. After the adsorption of BPA, a slight shift of carbonyl group peak from (532.0 eV) to higher binding energy (532.3 eV), which confirmed the aldehyde group of TpND for participating in the surface complexation through the formation of H-bonding (O...H). The content of O—H was increased (from 14.93% to 27.95%) due to the adsorption of BPA (Wei et al. 2020b). Indigo carmine dye has been successfully adsorbed on BTT-TAPT-COF by the presence of two significant characteristic peaks belonging to indigo carmine dye (sulfonate group in 168.3 eV and C=O in 287.8 eV) (Pan et al. 2020).

Theoretical calculation

To understand the interactions between organic pollutants and COFs, theoretical calculations such as density functional theory (DFT) and molecular simulation (MS) are used to determine the structure–property relationships, the charge density of the system, total energy information, and this investigates the adsorption behavior of organic pollutants that cannot be realized from experimental results and spectroscopic methods. These results can help researchers to design the structure of COFs/COF-based materials and optimize their adsorption performance (Wei et al. 2020a; Zhuang et al. 2020b).

Density function theory (DFT)

Density function theory (DFT) is a useful tool to explain the experimental results and spectroscopic analysis at the atomic level, such as orientations, lengths, bond energies, and the charge density of the system. The most significant advantage of DFT calculation is probing the species and microstructure at molecular levels under complicated conditions and the simulation of the interaction processes. For example, sulfamethazine molecules adsorbed in the pore-sites of

COFs through C–H $\cdots\pi$ interaction due to stable adsorption configuration while hydrogen bonding was not detected in this configuration (Zhuang et al. 2020b). To investigate the adsorption of bisphenol A to TpND the DFT calculation was used and it was found that bisphenol A is favorably removal by TpND phenolic aldehyde groups through the hydrogen bonds. Notably, the main electron transfer has occurred between the oxygen atoms (O1 and O2) in the phenolic aldehyde groups of TpND and the hydrogen atoms (H1 and H2) of BPA Which approved H-bonding interaction mechanisms during the sorption process (Wei et al. 2020b). DFT calculation of adsorption triphenyl phosphate on three COFs (COF1, COF2, COF3) with different pore sizes showed that the triphenyl phosphate could easily pretend into larger pore sizes (COF2 and COF3) and prevented from passing through the small pore size of COF1. This calculation explained the low adsorption capacity of triphenyl phosphate on COF1. However, with the easy diffusion of triphenyl phosphate into (COF2 and COF3), the larger pore size decrease the affinity of this molecule and increase the tendency to get-away outside (Wang et al. 2018c). pollutants and COFs at the molecular level, which are difficult to perform at experimental measurements.

DFT calculation of magnetic TPB-DMTP-COF for adsorption Ds and sulfamethazine molecules showed that these adsorbates were introduced into the TPB-DMTP-COF channel structure after adsorption. Both molecules were close to the π -wall of TPB-DMTP-COF, and their benzene ring structures were nearly vertical to that of TPB-DMTP-COF. The predominant interaction between layers to form the layered stacking structure was π - π interaction, and C-H $\cdots\pi$ interaction also contributed to the adsorption of diclofenac sodium/sulfamethazine into COFs (Zhuang et al. 2020a).

Molecular simulation

Molecular simulation (MS) is also a useful tool for determining the positions, the prediction of the macroscopic phenomena simulation, potential energies, describing the adsorption process at an atomic level, calculating driving forces and interaction energy of dynamic interactions (Hoskins & Robson 1989, Liu et al. 2021). MS simulation was used to study bisphenol A movement from the external solvent to the interior porous structure of TpND. Three different molecular numbers of BPA (Num 20, 10, and 5) were randomly settled in the box. For Num 20, the new peaks (around 9.78 nm, 11.94 nm) were embedded on the surface of TpND due to numerous BPA molecules would agglomerate into big clusters before they reached the surface of TpND and also the high volume and the big clusters were crowded by the hole-structure. For Num10, a portion of BPA molecules is assembled into the chain-type cluster and intercalated between the

inner layers. For Num 5, the BPA molecules could easily pretend into the surface and then be trapped in the interior of the TpND. Thus, the physical pore structure of COF and size of BPA cluster have a significant aggregating effect on the sorption process (Liu et al. 2021; Wei et al. 2020b).

Reports of molecular simulation studies on the elimination of organic contaminants by COFs are lower than those on gas adsorption due to the long-time of computational to simulate dense liquid phases. Hopefully more simulation studies on the removal of organic pollutants and deeper molecular insight as computational power increases. The computational simulation can help to understand the interaction processes of these pollutants and COFs at the molecular level, which are difficult to perform at experimental measurements.

Above all, spectroscopic techniques and theoretical calculations are used to confirm the adsorption mechanism and understand the interaction between COFs and organic contaminants. From XPS and FTIR spectra, the chemical shift proves the bonding information in the adsorption process of surface functional groups and molecular structures of adsorbents. On the other hand, DFT calculations approve these results from experimental techniques and explain the complicated relationship between sorption capacity and pore size. Moreover, MS can also assist the role of COFs in adsorption, electrostatic interactions, and ion exchange. Therefore, spectroscopic techniques and theoretical calculations play a major role in the mechanism study.

Comparison between COFs and other materials in removing organic pollutants

Table 6 tabulates the adsorption capacity of other materials for the elimination of organic pollutants. The recent studies of capturing PPCPs by COFs showed a significant adsorption capacity than other materials. For example, MCOF-2 showed higher adsorption capacity with faster adsorption kinetics and excellent reusability for removal diclofenac sodium than MOF-UiO-66, activated carbon from agricultural by-products, zeolitic imidazolate frameworks -8 PCDM-1000, carbide-derived carbons-1000, and Metal azolate framework-6-derived porous carbon-K1000. The high removal efficiency of DS by MCOFs was mainly caused by π - π stacking, electrostatic interaction, and hydrogen bonding interactions.

For adsorption SMT, TPB-DMTP-COF showed higher adsorption capacity with $q_{\max} = 209$ mg/g compared to mesoporous organosilica (Parambadath et al. 2016) and activated carbon (Yao et al. 2019) which agree that COF / COF based materials are an efficient absorbent for SMT removal. For removal IBU, it was noticed that the higher adsorption

capacity by TpBD-(CF₃)₂ focused on the advantage of using the fluorinated COF for pharmaceutical adsorption.

The reported studies for adsorption pesticides by COFs are very limited. However, the higher removal efficiency with more than 97% of methomyl, aldicarb, carbaryl, sulfide aldicarb, carbofuran, sulfone aldicarb, and imidacloprid by Fe₃O₄@SiO₂-NH₂@COFs, can't be holding a real comparison between COFs and other materials.

To date, an interesting adsorption capacity for cationic dye MEB by TS-COF-2 with $q_{\max} = 1691$ mg/g than amino-MIL-101(Al), nitrogen-doped porous carbon nanosheets-10, holey graphene nanosheets, ordered mesoporous carbon, porous carbon sheets, triptycene-based hyper-cross-linked polymer sponge and 1,4-dicyanobenzene polymer DCB2 see Table 6. COF-TzDBd showed higher adsorption capacity for capture CV and BG than other adsorbents such as Cd-MOF, zwitterionic polymer hydrogels, magnetite/silica/ pectin NPs, zero-valent iron anionic, and zeolite-MOF see Table 6.

For adsorption anionic dye, MO showed higher adsorption capacity by benzodimidazole-COF than activated carbon (Haque et al. 2011). The adsorption of neutral dye by COFs is used in a limited range. To understand the nature of the reaction between COFs and neutral dye isn't clear, it is necessary to use COFs as a platform to remove neutral dye such as NA, NR, and CA. DhaTab-PBA showed higher adsorption for elimination catechol than water-compatible hyper crosslinked resin HJ-1, hyper cross-linked Polymers, granular activated carbon, and Waste Fe (III) = Cr (III) Hydroxide.

Overall, COFs and COF-based materials showed higher efficiency than other materials due to high surface area, abundant functional groups, active sites, and appropriate pore size. COFs can be synthesized in green conditions with more active sites and ultrahigh porosity. In addition, they can be synthesized by novel methods with short preparation time and high yield. Multifunctional COFs platforms can be developed. Multi-component can be carried out through complex reactions with other functional composites.

Conclusion and perspectives

In summary, COFs can be considered as an alternative platform for the removal of different organic pollutants (pharmaceutical and personal care products, pesticides, dyes, and industrial by-products). In this review, different adsorption mechanisms were discussed considering the introduction of various functional groups such as N, O, and S into COFs. This remarkably improves the adsorption capacity due to the ability of these functional groups to form strong linkages with organic compounds. Moreover, the automerization of functional groups between two interconvertible structures (i.e., enamine-imine, ketone-enol, etc.) enhances the

adsorption performance. COFs are excellent adsorbents with high reusability, large adsorption capacities, and fast sorptive kinetics. For instance, the maximum adsorption capacity of methylene blue by COFs can be as high as 1691 mg g⁻¹, with rapid equilibrium time. Other studies have shown COFs capable of removing 565 mg g⁻¹ of diclofenac sodium. In addition, COF with 20% of amine loading has the highest affinity to ammonium perfluoro-2-propoxypropionate with maximum adsorption capacity = 240 mg g⁻¹. However, it is important to note that different structural designs of COFs influence the adsorption capacities, and the adsorption capacity of different contaminants by a particular COFs vary due to its pore structure, multiple functionalities, physical/chemical properties, selectivity as well as other process parameters such as pH.

The pore structure can be easily redesigned through various methods, suitable for the removal of different organic contaminants. Modification of COFs can combine the synergistic effects, chemical/physical properties, and multiple functionalities of the individual components. Furthermore, a short processing time with high yields can be achieved in the synthesis of COFs. 2D COFs have a high crystal structure and are more stable in different media (boiling water, organic solvent, acidic and basic conditions). However, the 2D COFs topological structural area is limited because of the limited pores design strategies associated with pore walls including distribution, intensity orientation, distribution, intensity, and alignment. Moreover, the addition of a new linker led to new topologies. It is very interesting to consider the pore size, and the shape of pores, to enhance the removal efficiency of emerging organic contaminants. In addition, COFs can be designed with favorite functionalities for definite applications. This selects the functional group of monomer and organic linkers in the synthesis process and post-synthetic modifications (PSM). As a result, COF influences the dimensionality, shape, surface area, pore size, and chemical conditions. Many COFs are used as a platform in bulk or nanosheet as well as a single adsorbent or in combinations to remove organic contaminants because of the open apertures and 1D channels free of chain entanglement and pore interpenetration, this enables full access to the porous space. Nevertheless, the stability of 3D COFs is a big challenge. Many 3D COFs like NPN-1, NPN-2, and NPN-3 have been synthesized. Still, the crystallinity and porosity cannot be determined by powder N₂ gas adsorption isotherms and powder X-ray diffraction, respectively, because of the instability of these COFs. Weak azodioxo bonds cause instability. In general, the stability is related to crystallinity and reverse to the reversible reaction. Moreover, synthesized single crystal 3D COFs were still lacking the diversity of the structure (not only imine linkage), limited in methodology (flow synthesis or vapor-assisted conversion,

Table 6 Various candidates and their maximum adsorption quantities (q_{\max} , mg g^{-1}) for the capture of organic contaminants

Organic contaminants	Adsorbent	Q_{\max} , mg g^{-1}	References
Pharmaceutical contaminants and personal care products (PPCPs)			
Diclofenac Na	MOF-UiO-66	189	(Lin et al. 2015)
	Activated carbon from agricultural by-products	56	(Larous & Meniai 2016)
	Zeolitic imidazolate frameworks -8 PCDM-1000	105	(Bhadra et al. 2017)
	Carbide-derived carbons-1000	351	(Álvarez-Torrellas et al. 2018)
	Metal azolate framework-6-derived porous carbon-K1000	503	(An et al. 2018)
Sulfamerazine	MA-PMO-5 / mesoporous organosilica	96	(Parambadath et al. 2016)
	SA-PMO-5/ mesoporous organosilica	31	(Parambadath et al. 2016)
	Granular activated carbon	165.67	(Yao et al. 2019)
Ibuprofen	Activated carbons / CAC	85.5	(Mestre et al. 2007)
	Activated carbons / CPAC	89.3	(Mestre et al. 2007)
	Activated carbon cloths	492	(Guedidi et al. 2017)
	Rice Straw Based Biochar	170	(Ahmed 2017)
	BiOCl microsphere	26.6	(Li et al. 2017)
	Magnetic palm-based powdered activated carbon- Triethoxyphenylsilane	100	(Wong et al. 2016)
	Magnetic carboxyl modified hyper cross-linked resins-10	0.8 mmol/g	(Jin et al. 2017)
	Magnetic carboxyl modified hyper cross-linked resins-10	0.7 mmol/g	(Jin et al. 2017)
	Magnetic carboxyl modified hyper cross-linked resins -30	0.6 mmol/g	(Jin et al. 2017)
	Magnetic carboxyl modified hyper cross-linked resins -30	0.45 mmol/g	(Jin et al. 2017)
	Magnetic carboxyl modified hyper cross-linked resins -40	0.1 mmol/g	(Jin et al. 2017)
	Magnetic carboxyl modified hyper cross-linked resins -50	0.059 – 1.3	(Reinholds et al. 2017)
	Magnetic carboxyl modified hyper cross-linked resins -70		
Multi-walled carbon nanotubes			
Pesticides			
Imidacloprid	Powdered Activated Carbon	110.59	(Zahoor et al. 2011)
	Magnetic Activated Carbon	94.89	(Zahoor et al. 2011)
Methylchlorophenoxy-propionic acid	MgAl-layered double hydroxides	0.08–1.21 mmol/g	(Inacio et al. 2001)
	Activated carbon	303	(Seo et al. 2015)
Chlorophenols	Multi-walled carbon nanotubes -OH	65	(Ding et al. 2016)
	Single-walled carbon nanotubes	84	(Ding et al. 2016)
	Multi-walled carbon nanotubes -COOH	65	(Ding et al. 2016)
	powdered activated carbon	81%	(Zhou et al. 2011)
	Granular Activated Carbon	294–467	(Hossain & McLaughlan 2012)
	Filter Coal	7–7.5	(Hossain & McLaughlan 2012)
	Pine	3.2–7	(Hossain & McLaughlan 2012)
Hardwood	3.5–7.4	(Hossain & McLaughlan 2012)	
Dimethyl phthalate	Single wall carbon nanotubes	148	(Wang et al. 2010)
	Activated Carbon-Cloth	2.25	(Ayranci & Bayram 2005)
	α -Cyclodextrin	2.76	(Chen et al. 2007)
	β -Cyclodextrin	1.8	(Murai et al. 1998)
Diethyl phthalate	Activated sludge	0.73	(Fang & Zheng 2004)
	Activated Carbon-Cloth	5.77	(Ayranci & Bayram 2005)
	Extracellular polymeric substances	14.3	(Fang & Zheng 2004)
Dibutyl phthalate	Activated sludge	17.6	(Fang & Zheng 2004)
	Extracellular polymeric substances	10.6	(Fang & Zheng 2004)
	alkylbenzene-functionalized	184.9	(Zhang et al. 2018a)
2,4-Dichlorophenoxy-acetic acid (2,4-D)	Activated carbon	286	(Sarker et al. 2017)
	Zeolite USY	256	(Sarker et al. 2017)
	Granulated activated carbon	182	(Salman & Hameed 2010)
Organic dyes			
Rhodamine -B	Jack fruit peel activated carbon	85.9%	(Sivamani & Leena 2009)
	Tapioca peel activated carbon	88.2%	(Inbaraj & Sulochana 2006)
	Sodium Montmorillonite	42.19	(Selvam et al. 2008)

Table 6 (continued)

Organic contaminants	Adsorbent	Q_{\max} , mg g ⁻¹	References
Crystal violet CV	Cd-MOF	221	(Chand et al. 2017)
	Anionic zeolite-MOF	270	(Shen et al. 2016)
	Fe-MOF	812	(Sarker et al. 2019)
	Zwitterionic polymer hydrogels	13.5	(Rehman et al. 2019)
	Magnetite/silica/pectin NPs	125	(Attallah et al. 2016)
	Zero-valent iron	172	(Liu et al. 2018a)
Methyl orange	Activated carbon	11.2	(Haque et al. 2011)
Methylene Blue	ZJU-24-MOF	902	(Zhang et al. 2014)
	H ₃ PW ₁₂ O ₄₀ C ZIF-8 (BIT-1)	810	(Li et al. 2014)
	Amino-MIL-101(AI)	762	(Haque et al. 2014)
	Nitrogen-doped porous carbon nanosheets-10	962	(Gong et al. 2016)
	Holey graphene nanosheets	269	(Xing et al. 2014)
	Ordered mesoporous carbon	758	(Zhuang et al. 2009)
	Porous Carbon sheets	769	(Gong et al. 2015)
	Triptycene-based hyper-cross-linked polymer sponge	330	(Zhang et al. 2015)
		351	(Kuhn et al. 2008)
		1,4-dicyanobenzene polymer DCB2	
Industrial organic contaminants			
Catechol	Granular activated carbon	100	(Suresh et al. 2011)
	Water-compatible hyper crosslinked resin HJ-1	99	(Huang et al. 2009)
	Hyper cross-linked Polymers	55	(Sun et al. 2005)
	Waste Fe (III) = Cr (III) Hydroxide	4	(Namasivayam et al. 2004)
Phenol	Activated carbon	293	(Girods et al. 2009)
	Activated carbon fiber (ACF)	110	(Liu et al. 2010)
	MIL-53(Cr)	267	(Maes et al. 2011)
	Polyacrylonitrile /activated carbon	77	(Laszlo et al. 2003)
p-Nitrophenol	Silica beads	116	(Phan et al. 2000)
	Nanocrystalline hydroxyapatite	8.9	(Wei et al. 2010)
	Bagasse fly ash	8.3	(Dhaka et al. 2019)

mechanochemical synthesis), and the absence of additional driving force (mainly π - π stackings).

Hence, there are many challenges in the application of COFs for water treatment. Some of these challenges include 1) the stability of COFs in acidic, basic conditions, real, synthetic water under, liquid systems and air exposures, (Existing studies discussed the effect of pH, temperature, concentration- but only a few consider real water investigations such as tap water, and river water (generally ranging from ng L⁻¹ to μ g L⁻¹), or even a mixture of them, 2) The safety of materials, the synthetic conditions (preferably the nontoxic conditions) are essential for industrial applications in real water treatment, 3) high-cost of synthetic materials, 4) difficulty in recyclability and reusability, for instance, most research studies only consider the regeneration for short-term use while the long-term use was neglected, 5) Moreover, the removal of organic contaminants is still limited. For example, the simultaneous adsorption and degradation of pollutants by COFs should be studied, 6) Due to the uncertain relationship between the structure, performance, and mechanism of COF materials. It is highly recommended to calculate the in situ DFT and EXAFS, XPS, XRD, and other advanced spectroscopic techniques to detect the reaction process to distinguish reactive intermediates from the

active site. Overall, these problems should be considered in future studies. We also anticipate the synthesis of a wide range of COF materials which will increase its depth of application in environmental remediation.

Abbreviations

COFs	covalent organic frameworks	PAEs	phthalic acid esters
2D	two-dimensional	PUHs	phenyl urea herbicides
3D	three-dimensional	EDCs	endocrine disruptor chemicals
MOFs	metal-organic frameworks	Bus	benzoylurea insecticides
MO	methyl orange	RhB	rhodamine B
MB	methyl blue	CV	crystal violet
AG	acid green 25	DMPD	N, N-Dimethyl-P-Phenylenediamine dihydrochloride
DFBM	direct fast brown M	BG	brilliant green
IC	indigo carmine	MEB	methylene blue
AR-27	acid red 27	BEN	benzene

Abbreviations

PPCPs	pharmaceutical, personal care products	PHOL	phenol
STPs	sewage treatment plants	AN	aniline
WWTPs	wastewater treatment plants	BS	benzenesulfonate
AOPs	advanced oxidation processes	NB	nitrobenzene
SMZ	sulfamethoxazole	DNB	1,3-Dinitrobenzene
SIZ	sulfafurazole	TNB	1,3,5-Trinitrobenzene
SMT	sulfamethazine	MDNP	4-Ethyl-2,6-Dinitrophenol
ENX	enrofloxacin	NAPH	Naphthalene
DAN	danofloxacin	2-NAOL	2-Naphthol
ORB	orbifloxacin	1-NALA	1-Naphthalenamine
OFL	ofloxacin	2-NS	2-Naphthalenesulfonate
ENO	enoxacin	EDA	Electron-donor-acceptor
CIP	ciprofloxacin	BPA	Bisphenol A
IBU	ibuprofen	BPB	Bisphenol B
DS	diclofenac sodium	BPC	Bisphenol C
KT	ketoprofen	PFAS	polyfluorinated alkyl substances
IDM	indomethacin	PFOA	perfluorooctanoic acid
GO	graphene oxide	PFO	perfluorooctane sulfonate
NPX	naproxen	GenX	ammonium perfluoro-2 propoxypropionate
ACE	acetaminophen	AFFF	film-forming foams
FQs	fluoroquinolones		

Acknowledgements The authors are grateful for the availability of literature materials by Huazhong University of Science and Technology. The first author is also grateful for financial support from the China Scholarship Council.

Author contribution Author contributions to the present paper are as follows: Eman Abdelnasser Gendy—investigation, Conceptualization, Methodology, Visualization, Writing—Original draft, Writing—Review & Editing. Daniel Temitayo Oyekunle—investigation and validation. Jerosha Ifthikar—Resources. Ali Jawad—Resources. Zhuqi Chen—Supervision, Writing—Review & Editing.

Data availability There is no data or materials associated with this submission.

Declarations

Ethical approval and consent to participate Not applicable.

Consent for publication Not applicable.

Conflict of interest The authors declare no competing interests.

References

- Ahmed MJ (2017) Adsorption of non-steroidal anti-inflammatory drugs from aqueous solution using activated carbons. *J Environ Manage* 190:274–282. <https://doi.org/10.1016/j.jenvman.2016.12.073>
- Al-Shannag M, Al-Qodah Z, Bani-Melhem K, Qtaishat MR, Alkasrawi M (2015) Heavy metal ions removal from metal plating wastewater using electrocoagulation: Kinetic study and process performance. *Chem Eng J* 260:749–756. <https://doi.org/10.1016/j.cej.2014.09.035>
- Álvarez-Torrellas S, Muñoz M, Gläsel J, De Pedro ZM, Domínguez CM, García J, Etzold BJ, Casas JA (2018) Highly efficient removal of pharmaceuticals from water by well-defined carbide-derived carbons. *Chem Eng J* 347:595–606. <https://doi.org/10.1016/j.cej.2018.04.127>
- Amirilargani M, Merlet RB, Hedayati P, Nijmeijer A, Winnubst L, De Smet LC, Sudhölter E (2019): MIL-53 (Al) and NH 2-MIL-53 (Al) modified α -alumina membranes for efficient adsorption of dyes from organic solvents. *Chem. Comm.* 55, 4119–4122. <https://doi.org/10.1039/C9CC01624D>
- An HJ, Bhadra BN, Khan NA, Jung SH (2018) Adsorptive removal of wide range of pharmaceutical and personal care products from water by using metal azolate framework-6-derived porous carbon. *Chem Eng J* 343:447–454. <https://doi.org/10.1016/j.cej.2018.03.025>
- Attallah OA, Al-Ghobashy MA, Nebsen M, Salem MY (2016) Removal of cationic and anionic dyes from aqueous solution with magnetite/pectin and magnetite/silica/pectin hybrid nanocomposites: kinetic, isotherm and mechanism analysis. *RSC Adv* 6:11461–11480. <https://doi.org/10.1039/C5RA23452B>
- Ayranci E, Bayram E (2005) Adsorption of phthalic acid and its esters onto high-area activated carbon-cloth studied by in situ UV-spectroscopy. *J Hazard Mater* 122:147–153. <https://doi.org/10.1016/j.jhazmat.2005.03.022>
- Azzouz A, Ballesteros E (2012) Combined microwave-assisted extraction and continuous solid-phase extraction prior to gas chromatography—Mass spectrometry determination of pharmaceuticals, personal care products and hormones in soils, sediments and sludge. *Sci Total Environ* 419:208–215. <https://doi.org/10.1016/j.scitotenv.2011.12.058>
- Bagheri AR, Aramesh N, Sher F, Bilal M (2021) Covalent organic frameworks as robust materials for mitigation of environmental pollutants. *Chemosphere* 270:129523. <https://doi.org/10.1016/j.chemosphere.2020.129523>
- Bhadra BN, Ahmed I, Kim S, Jung SH (2017) Adsorptive Removal of Ibuprofen and Diclofenac from Water Using Metal-Organic Framework-Derived Porous Carbon 314:50–58. <https://doi.org/10.1016/j.cej.2016.12.127>
- Bisbey RP, Dichtel W (2017) Covalent organic frameworks as a platform for multidimensional polymerization. *Chem Eng J* 3:533–543. <https://doi.org/10.1016/j.cej.2016.12.127>
- Brutti M, Blasco C, Picó Y (2010) Determination of benzoylurea insecticides in food by pressurized liquid extraction and LC-MS. *J Sep Sci* 3(3):1–10. <https://doi.org/10.1002/jssc.200900314>
- Bu Q, Wang B, Huang J, Deng S, Yu G (2013) Pharmaceuticals and personal care products in the aquatic environment in China: a review. *J Hazard Mater* 262:189–211. <https://doi.org/10.1002/3527601856>

- Buchmeiser MRJPMiOS, Catalysis, , 2003 Buchmeiser MRJPMiOS, Catalysis, 2003 Metathesis-based polymers for organic synthesis and catalysis Poly Mater Organ Synth and Catal 346 <https://doi.org/10.1002/3527601856>
- Cabral JPJJoer, health p, (2010) Water microbiology. Bacterial pathogens and water. *Int J Environ Res Public* 7:3657–3703. <https://doi.org/10.3390/ijerph7103657>
- Cao S, Li B, Zhu R, Pang H (2019) Design and synthesis of covalent organic frameworks towards energy and environment fields. *Chem Eng J* 355:602–623. <https://doi.org/10.1016/j.cej.2018.08.184>
- Chand S, Elahi SM, Pal A, Das MC (2017) A new set of Cd (ii)-coordination polymers with mixed ligands of dicarboxylate and pyridyl substituted diaminotriazine: selective sorption towards CO 2 and cationic dyes. *Dalton Trans* 46:9901–9911. <https://doi.org/10.1039/C7DT01657C>
- Chaudhry MT, Zohaib M, Rauf N, Tahir SS, Parvez S (2014) Biosorption characteristics of *Aspergillus fumigatus* for the decolorization of triphenylmethane dye acid violet 49. *Appl Microbiol Biotechnol* 98:3133–3141. <https://doi.org/10.1007/s00253-013-5306-y>
- Chen C-Y, Chen C-C, Chung Y-C (2007) Removal of phthalate esters by α -cyclodextrin-linked chitosan bead. *Bioresour Technol* 98:2578–2583. <https://doi.org/10.1016/j.biortech.2006.09.009>
- Chen SH, Ting ASY (2015) Biodecolorization and biodegradation potential of recalcitrant triphenylmethane dyes by *Coriopsis* sp. isolated from compost. *J Environ Manage* 150:274–280. <https://doi.org/10.1016/j.jenvman.2014.09.014>
- Chen X, Geng K, Liu R, Tan KT, Gong Y, Li Z, Tao S, Jiang Q, Jiang D (2020) Covalent Organic Frameworks: Chemical Approaches to Designer Structures and Built-In Functions. *Angew Chem* 59:5050–5091. <https://doi.org/10.1002/anie.201904291>
- Das S, Heasman P, Ben T, Qiu S (2017) Porous organic materials: strategic design and structure–function correlation. *Chem Rev* 117:1515–1563. <https://doi.org/10.1021/acs.chemrev.6b00439>
- Davarnejad R, Soofi B, Farghadani F, Behfar R (2018) Ibuprofen removal from a medicinal effluent: A review on the various techniques for medicinal effluents treatment. *Environ Technol Innov* 11:308–320. <https://doi.org/10.1016/j.eti.2018.06.011>
- Dhaka S, Kumar R, Deep A, Kurade MB, Ji S-W, Jeon B-H (2019) Metal–organic frameworks (MOFs) for the removal of emerging contaminants from aquatic environments. *Chem Rev* 380:330–352. <https://doi.org/10.1021/acs.chemrev.9b00797>
- Ding H, Li X, Wang J, Zhang X, Chen CJ (2016) Adsorption of chlorophenols from aqueous solutions by pristine and surface functionalized single-walled carbon nanotubes. *J Environ Sci* 43:187–198. <https://doi.org/10.1016/j.jes.2015.09.004>
- Erogul S, Bas SZ, Ozmen M, Yildiz S (2015) A new electrochemical sensor based on Fe₃O₄ functionalized graphene oxide-gold nanoparticle composite film for simultaneous determination of catechol and hydroquinone. *Electrochim Acta* 186:302–313. <https://doi.org/10.1016/j.electacta.2015.10.174>
- Fang HH, Zheng H (2004) Adsorption of phthalates by activated sludge and its biopolymers. *Environ Technol* 25:757–761. <https://doi.org/10.1080/09593330.2004.9619366>
- Fang Q, Zhuang Z, Gu S, Kaspar RB, Zheng J, Wang J, Qiu S, Yan Y (2014) Designed synthesis of large-pore crystalline polyimide covalent organic frameworks. *Nat Commun* 5:1–8. <https://doi.org/10.1038/ncomms5503>
- Feng X, Fryxell GE, Wang L-Q, Kim AY, Liu J, Kemner KM (1997) Functionalized monolayers on ordered mesoporous supports. *Chem Rev* 276:923–926. <https://doi.org/10.1021/acs.chemrev.9b00550>
- Gendy et al., 2021a EA Gendy J Ifthikar J Ali DT Oyekunle Z Elkhilifa II Shahib AI Khodair ZJ Chen 2021a Removal of heavy metals by Covalent Organic Frameworks (COFs): A review on its mechanism and adsorption properties *J Environ Chem Eng* 105687 <https://doi.org/10.1016/j.jece.2021.105687>
- Gendy EA, Oyekunle DT, Ali J, Ifthikar J, Ramadan AE-MM, Chen ZJJoER, (2021b) High-performance removal of radionuclides by porous organic frameworks from the aquatic environment: A review. *J Environ Radioact* 238:106710. <https://doi.org/10.1016/j.jenvrad.2021.106710>
- Geng K, He T, Liu R, Dalapati S, Tan KT, Li Z, Tao S, Gong Y, Jiang Q (2020) Jiang D (2020a): Covalent Organic Frameworks: Design, Synthesis, and Functions. *Chem Rev* 120(16):8814–8933. <https://doi.org/10.1021/acs.chemrev.9b00550>
- Girods P, Dufour A, Fierro V, Rogaume Y, Rogaume C, Zoulalian A, Celzard A (2009) Activated carbons prepared from wood particleboard wastes: Characterisation and phenol adsorption capacities. *J Hazard Mater* 166:491–501. <https://doi.org/10.1016/j.jhazmat.2008.11.047>
- Gong J, Liu J, Chen X, Jiang Z, Wen X, Mijowska E, Tang T (2015) Converting real-world mixed waste plastics into porous carbon nanosheets with excellent performance in the adsorption of an organic dye from wastewater. *J Mater Chem a* 3:341–351. <https://doi.org/10.1039/C4TA05118A>
- Gong J, Lin H, Antonietti M, Yuan J (2016) Nitrogen-doped porous carbon nanosheets derived from poly (ionic liquid) s: hierarchical pore structures for efficient CO 2 capture and dye removal. *J Mater Chem a* 4:7313–7321. <https://doi.org/10.1039/C3TA13589F>
- Guedidi H, Reinert L, Soneda Y, Bellakhal N, Duclaux L (2017) Adsorption of ibuprofen from aqueous solution on chemically surface-modified activated carbon cloths. *Arab J Chem* 10:S3584–S3594. <https://doi.org/10.1016/j.arabjc.2014.03.007>
- Hao J, Zhang Q, Chen P, Zheng X, Wu Y, Ma D, Wei D, Liu H, Liu G, Lv W (2019) Removal of pharmaceuticals and personal care products (PPCPs) from water and wastewater using novel sulfonic acid (–SO 3 H) functionalized covalent organic frameworks. *Environ Sci* 6:3374–3387. <https://doi.org/10.1039/C9EN00708C>
- Haque E, Jun JW, Jung SH (2011) Adsorptive removal of methyl orange and methylene blue from aqueous solution with a metal-organic framework material, iron terephthalate (MOF-235). *J Hazard Mater* 185:507–511. <https://doi.org/10.1039/C8RA10429H>
- Haque E, Lo V, Minett AI, Harris AT, Church TL (2014) Dichotomous adsorption behaviour of dyes on an amino-functionalised metal–organic framework, amino-MIL-101 (Al). *J Mater Chem a* 2:193–203. <https://doi.org/10.1039/C3TA13589F>
- Hasan Z, Jung SH (2015) Removal of hazardous organics from water using metal-organic frameworks (MOFs): plausible mechanisms for selective adsorptions. *J Hazard Mater* 283:329–339. <https://doi.org/10.1016/j.jhazmat.2014.09.046>
- Hassaan MA, El Nemr AJA, Engineering (2017): Health and environmental impacts of dyes: mini review. *J. Environ. Sci.* 1, 64–67. <https://doi.org/10.11648/j.ajese.20170103.11>
- Heydaripour J, Gazi M, Oladipo AA, Gulcan HO (2019) Porous magnetic resin-g-chitosan beads for adsorptive removal of phenolic compounds. *Int J Biol Macromol* 123:1125–1131. <https://doi.org/10.1016/j.ijbiomac.2018.11.168>
- Hoskins BF, Robson R (1989) Infinite polymeric frameworks consisting of three dimensionally linked rod-like segments. *J Am Chem Soc* 111:5962–5964. <https://doi.org/10.1021/ja00197a079>
- Hossain G, McLaughlan R (2012) Sorption of chlorophenols from aqueous solution by granular activated carbon, filter coal, pine and hardwood. *Environ Technol* 33:1839–1846. <https://doi.org/10.1016/j.jes.2015.09.004>

- Hou Y, Zhang X, Wang C, Qi D, Gu Y, Wang Z, Jiang J (2017) Novel imine-linked porphyrin covalent organic frameworks with good adsorption removing properties of RhB. *New J Chem* 41:6145–6151. <https://doi.org/10.1039/C7NJ00424A>
- Hu B, Ai Y, Jin J, Hayat T, Alsaedi A, Zhuang L, Wang X (2020a) Efficient elimination of organic and inorganic pollutants by biochar and biochar-based materials. *Biochar* 2:47–64. <https://doi.org/10.1021/jacs.8b06958>
- Hu X, Xu G, Zhang H, Li M, Tu Y, Xie X, Zhu Y, Jiang L, Zhu X, Ji X (2020b) Multifunctional β -cyclodextrin polymer for simultaneous removal of natural organic matter and organic micropollutants and detrimental microorganisms from water. *ACS Appl Mater Interfaces* 12:12165–12175. <https://doi.org/10.1021/acsami.0c00597>
- Huang J, Huang K, Yan C (2009) Application of an easily water-compatible hypercrosslinked polymeric adsorbent for efficient removal of catechol and resorcinol in aqueous solution. *J Hazard Mater* 167:69–74. <https://doi.org/10.1016/j.jhazmat.2008.12.120>
- Huang L, Mao N, Yan Q, Zhang D, Shuai Q (2019) Magnetic Covalent Organic Frameworks for the Removal of Diclofenac Sodium from Water. *ACS Appl Nano Mater* 3(1):319–326. <https://doi.org/10.1021/acsanm.9b01969>
- Huang N, Wang P, Jiang, (2016) Covalent organic frameworks: a materials platform for structural and functional designs. *Nat Rev Mater* 1:1–19. <https://doi.org/10.1038/natrevmats.2016.68>
- Huang N, Zhai L, Xu H, Jiang D (2017) Stable covalent organic frameworks for exceptional mercury removal from aqueous solutions. *J Am Chem Soc* 139:2428–2434. <https://doi.org/10.1021/jacs.6b12328>
- Huo J, Luo B, Chen Y (2019) Crystalline Covalent Organic Frameworks from Triazine Nodes as Porous Adsorbents for Dye Pollutants. *ACS Omega* 4(27):22504–22513. <https://doi.org/10.1021/acsomega.9b03176>
- Inacio J, Taviot-Gueho C, Forano C, Besse J (2001) Adsorption of MCPA pesticide by MgAl-layered double hydroxides. *Appl Clay Sci* 18:255–264. [https://doi.org/10.1016/S0169-1317\(01\)00029-1](https://doi.org/10.1016/S0169-1317(01)00029-1)
- Inbaraj BS, Sulochana N (2006) Use of jackfruit peel carbon (JPC) for adsorption of rhodamine-B, a basic dye from aqueous solution. <http://hdl.handle.net/123456789/6990>
- Ji S-L, Qian H-L, Yang C-X, Zhao X, Yan X-P (2019a) Thiol-Ene Click Synthesis of Phenylboronic Acid-Functionalized Covalent Organic Framework for Selective Catechol Removal from Aqueous Medium. *ACS Appl Mater Interfaces* 11:46219–46225
- Ji W-H, Guo Y-S, Wang X, Lu X-F, Guo D-S (2019b) Amino-modified covalent organic framework as solid phase extraction adsorbent for determination of carboxylic acid pesticides in environmental water samples. *J Chromatogr A* 1595:11–18. <https://doi.org/10.1021/acsomega.9b0317>
- Ji W, Xiao L, Ling Y, Ching C, Matsumoto M, Bisbey RP, Helbling DE, Dichtel WR (2018) Removal of GenX and perfluorinated alkyl substances from water by amine-functionalized covalent organic frameworks. *J Am Chem Soc* 140:12677–12681. <https://doi.org/10.1021/jacs.8b06958>
- Jiang J-J, Lee C-L, Fang M-D (2014) Emerging organic contaminants in coastal waters: anthropogenic impact, environmental release and ecological risk. *Mar Pollut Bull* 85:391–399. <https://doi.org/10.1016/j.marpolbul.2013.12.045>
- Jin J, Feng T, Ma Y, Wang W, Wang Y, Zhou Q, Li AJC (2017) Novel magnetic carboxyl modified hypercrosslinked resins for effective removal of typical PPCPs. *Chemosphere* 185:563–573. <https://doi.org/10.1016/j.chemosphere.2017.07.058>
- Khodadadi M, Ehrampoush M, Ghaneian M, Allahresani A, Mahvi A (2018) Synthesis and characterizations of FeNi₃@ SiO₂@ TiO₂ nanocomposite and its application in photo-catalytic degradation of tetracycline in simulated wastewater. *J Mol Liq* 255:224–232. <https://doi.org/10.1016/j.molliq.2017.11.137>
- Kråkström et al., 2021 M Kråkström S Saeid P Tolvanen N Kumar T Salmi L Kronberg P Eklund Engineering, 2021 Identification and Quantification of Transformation Products Formed during the Ozonation of the Non-steroidal Anti-inflammatory Pharmaceuticals Ibuprofen and Diclofenac *Ozone Sci Eng* 1–15 <https://doi.org/10.1080/01919512.2021.1898928>
- Kuhn et al., 2008 P Kuhn K Krüger A Thomas M Antonietti 2008 “Everything is surface”: tunable polymer organic frameworks with ultrahigh dye sorption capacity *Chem Comm* 5815 5817 <https://doi.org/10.1039/B814254H>
- Lam B, Déon S, Morin-Crini N, Crini G, Fievet P (2018) Polymer-enhanced ultrafiltration for heavy metal removal: Influence of chitosan and carboxymethyl cellulose on filtration performances. *J Clean Prod* 171:927–933. <https://doi.org/10.1016/j.jclepro.2017.10.090>
- Larous S, Meniai A.H (2016) Adsorption of Diclofenac from aqueous solution using activated carbon prepared from olive stones. *Chemosphere* 41:10380–10390. <https://doi.org/10.1016/j.chemosphere.2018.11.023>
- Laszlo K, Podkościelny P, Dabrowski A (2003) Heterogeneity of polymer-based active carbons in adsorption of aqueous solutions of phenol and 2, 3, 4-trichlorophenol. *Langmuir* 19:5287–5294. <https://doi.org/10.1021/la026761s>
- Li J, Sun S, Chen R, Zhang T, Ren B, Dionysiou DD, Wu Z, Liu X, Ye M (2017) Adsorption behavior and mechanism of ibuprofen onto BiOCl microspheres with exposed 001 facets. *Environ Sci Pollut Res* 24:9556–9565
- Li R, Ren X, Zhao J, Feng X, Jiang X, Fan X, Lin Z, Li X, Hu C, Wang B (2014) Polyoxometallates trapped in a zeolitic imidazolate framework leading to high uptake and selectivity of bioactive molecules. *J Environ Manage* 2:2168–2173. <https://doi.org/10.1016/j.jenvman.2016.12.073>
- Li W, Jiang H-X, Geng Y, Wang X-H, Gao R-Z, Tang A-N, Kong D-M (2020a) Facile Removal of Phytochromes and Efficient Recovery of Pesticides Using Heteropore Covalent Organic Framework-Based Magnetic Nanospheres and Electrospun Films. *ACS Appl Mater Interfaces* 12:20922–20932. <https://doi.org/10.1021/acsami.0c01608>
- Li Y, Cui W, Liu L, Zong R, Yao W, Liang Y, Zhu YJACBE (2016) Removal of Cr (VI) by 3D TiO₂-graphene hydrogel via adsorption enriched with photocatalytic reduction. *Appl Catal B* 199:412–423. <https://doi.org/10.1016/j.apcatb.2016.06.053>
- Li Y, Chen W, Hao W, Li Y, Chen L (2018) Covalent organic frameworks constructed from flexible building blocks with high adsorption capacity for pollutants. *ACS Appl Nano Mater* 1:4756–4761. <https://doi.org/10.1021/acsanm.8b00983>
- Li Y, Yang C-X, Qian H-L, Zhao X, Yan X-P (2019a) Carboxyl-Functionalized Covalent Organic Frameworks for the Adsorption and Removal of Triphenylmethane Dyes. *ACS Appl Nano Mater* 2:7290–7298. <https://doi.org/10.1021/acsanm.9b01781>
- Li Y, Zhang H, Chen Y, Huang L, Lin Z, Cai Z (2019b) Core-shell structured magnetic covalent organic framework nanocomposites for triclosan and triclocarban adsorption. *ACS Appl Mater Interfaces* 11:22492–22500. <https://doi.org/10.1007/s00604-018-3198-3>
- Li Z, Liu Y, Zou S, Lu C, Bai H, Mu H, Duan J (2020b) Removal and adsorption mechanism of tetracycline and cefotaxime contaminants in water by NiFe₂O₄-COF-chitosan-terephthalaldehyde nanocomposites film. *Chem Eng J* 382:123008. <https://doi.org/10.1016/j.cej.2019.123008>
- Liang XX, Omer A, Hu Z-h, Wang Yg YuD, Ouyang X-k (2019) Efficient adsorption of diclofenac sodium from aqueous solutions using magnetic amine-functionalized chitosan. *Chemosphere* 217:270–278. <https://doi.org/10.1016/j.chemosphere.2018.11.023>

- Lin K-YA, Yang H, Lee W-D (2015) Enhanced removal of diclofenac from water using a zeolitic imidazole framework functionalized with cetyltrimethylammonium bromide (CTAB). *J Hazard Mater* 5:81330–81340. <https://doi.org/10.1016/j.jhazmat.2010.09.035>
- Liu H, Sun R, Feng S, Wang D, Liu H (2019): Rapid synthesis of a silsesquioxane-based disulfide-linked polymer for selective removal of cationic dyes from aqueous solutions. 359, 436–445. *Chem. Eng. J.* <https://doi.org/10.1016/j.cej.2018.11.148>
- Liu J, Zong E, Fu H, Zheng S, Xu Z, Zhu D (2012) Adsorption of aromatic compounds on porous covalent triazine-based framework. *J Colloid Interface Sci* 372:99–107. <https://doi.org/10.1016/j.jcis.2012.01.011>
- Liu J, Wang Y, Fang Y, Mwamulima T, Song S, Peng C (2018a) Removal of crystal violet and methylene blue from aqueous solutions using the fly ash-based adsorbent material-supported zero-valent iron. *J Mol Liq* 250:468–476. <https://doi.org/10.1016/j.molliq.2017.12.003>
- Liu Q-S, Zheng T, Wang P, Jiang J-P, Li N (2010): Adsorption isotherm, kinetic and mechanism studies of some substituted phenols on activated carbon fibers. 157, 348–356. *Chem. Eng. J.* <https://doi.org/10.1016/j.cej.2009.11.013>
- Liu et al., 2021 X Liu H Pang X Liu Q Li N Zhang L Mao M Qiu B Hu H Yang X Wang 2021 Orderly porous covalent organic frameworks-based materials: superior adsorbents for pollutants removal from aqueous solutions *Innov J* 100076 <https://doi.org/10.1016/j.xinn.2021.100076>
- Liu Y, Gao M, Gu Z, Luo Z, Ye Y, Lu L (2014) Comparison between the removal of phenol and catechol by modified montmorillonite with two novel hydroxyl-containing Gemini surfactants. *J Hazard Mater* 267:71–80. <https://doi.org/10.1016/j.jhazmat.2013.12.039>
- Liu Y, Fan Q, Wang J (2018b): Zn-Fe-CNTs catalytic in situ generation of H₂O₂ for Fenton-like degradation of sulfamethoxazole. *J. Hazard. Mater.* 342, 166–176. <https://doi.org/10.1016/j.jhazmat.2017.08.016>
- Lohse MS, Stassin T, Naudin G, Wuttke S, Ameloot R, De Vos D, Medina DD, Bein T (2016) Sequential pore wall modification in a covalent organic framework for application in lactic acid adsorption. *Chem Mater* 28:626–631. <https://doi.org/10.1021/acs.chemmater.5b04388>
- Lushchak VI, Matviishyn TM, Husak VV, Storey JM, Storey KB (2018): Pesticide toxicity: a mechanistic approach. *EXCLI J.* 17, 1101. <https://doi.org/10.17179/excli2018-1710>
- Lv S-W, Liu J-M, Wang Z-H, Ma H, Li C-Y, Zhao N, Wang SJJoes (2019): Recent advances on porous organic frameworks for the adsorptive removal of hazardous materials. 80, 169–185. *Chem. Eng. J.* <https://doi.org/10.1016/j.cej.2014.09.035>
- Maes M, Schouteden S, Alaerts L, Depla D, De Vos DEJPCCP (2011) Extracting organic contaminants from water using the metal-organic framework Cr III (OH)·{O 2 C-C 6 H 4-CO 2}. *Phys Chem Chem Phys* 13:5587–5589. <https://doi.org/10.1039/C0CP01703E>
- Meffe R, de Bustamante I (2014): Emerging organic contaminants in surface water and groundwater: a first overview of the situation in Italy. 481, 280–295. *Sci. Total Environ.* <https://doi.org/10.1016/j.scitotenv.2014.02.053>
- Mellah A, Fernandes SP, Rodríguez R, Otero J, Paz J, Cruces J, Medina DD, Djamila H, Espiña B, Salonen LM (2018) Adsorption of pharmaceutical pollutants from water using covalent organic frameworks. *Chem Eur J* a 24:10601–10605. <https://doi.org/10.1002/chem.201801649>
- Mestre A, Pires J, Nogueira J, Carvalho A (2007) Activated carbons for the adsorption of ibuprofen. *Carbon* 45:1979–1988. <https://doi.org/10.1016/j.carbon.2007.06.005>
- Mon M, Bruno R, Ferrando-Soria J, Armentano D, Pardo E (2018) Metal-organic framework technologies for water remediation: towards a sustainable ecosystem. *J Mater Chem* a 6:4912–4947. <https://doi.org/10.1021/acsomega.9b0317>
- Mori T, Inoue Y (2005) Circular Dichroism of a Chiral Tethered Donor-Acceptor System: Enhanced Anisotropy Factors in Charge-Transfer Transitions by Dimer Formation and by Confinement. *Angew Chem* 44:2582–2585. <https://doi.org/10.1002/anie.200462071>
- Murai S, Imajo S, Takasu Y, Takahashi K, Hattori K (1998) Removal of phthalic acid esters from aqueous solution by inclusion and adsorption on β-cyclodextrin. *Environ Sci Technol* 32:782–787. <https://doi.org/10.1021/es970463d>
- Nagpal M, Kakkar R (2019) Use of metal oxides for the adsorptive removal of toxic organic pollutants. *Sep Purif Technol* 211:522–539. <https://doi.org/10.1016/j.seppur.2018.10.016>
- Namasivayam C, Sumithra SJI, research ec, (2004) Adsorptive removal of catechol on waste Fe (III)/Cr (III) hydroxide: equilibrium and kinetics study. *Ind Eng Chem Res* 43:7581–7587. <https://doi.org/10.1021/ie0496636>
- Nde SC, Mathuthu MJIjoer, health p, (2018) Assessment of Potentially Toxic Elements as Non-Point Sources of Contamination in the Upper Crocodile Catchment Area, North-West Province, South Africa. *Int J Environ Res Public* 15:576. <https://doi.org/10.3390/ijerph15040576>
- Nguyen TA, Juang R-S (2013) Treatment of waters and wastewaters containing sulfur dyes: a review. *Chem Eng J* 219:109–117. <https://doi.org/10.1016/j.cej.2012.12.102>
- Nieder R, Benbi DK, Reichl FX (2018): Role of potentially toxic elements in soils, Soil Components and Human Health. *Soil components and human health.* Springer, pp. 375–450. https://doi.org/10.1007/978-94-024-1222-2_8
- Oba et al., 2021 SN Oba JO Ighalo CO Aniagor CA Igwegbe 2021 Removal of ibuprofen from aqueous media by adsorption: A comprehensive review *Sci Total Environ* 146608 <https://doi.org/10.1016/j.scitotenv.2021.146608>
- Pan et al., 2020 X Pan X Qin Q Zhang Y Ge H Ke G Cheng 2020 N-and S-rich covalent organic framework for highly efficient removal of indigo carmine and reversible iodine capture *Microporous Mesoporous Mater* 109990 <https://doi.org/10.1016/j.micromeso.2019.109990>
- Parambadath S, Mathew A, Barnabas MJ, Rao KM, Ha C-S (2016) Periodic mesoporous organosilica (PMO) containing bridged succinamic acid groups as a nanocarrier for sulfamerazine, sulfadiazine and famotidine: Adsorption and release study. *Microporous Mesoporous Mater* 225:174–184. <https://doi.org/10.1016/j.micromeso.2015.12.016>
- Peligro FR, Pavlovic I, Rojas R, Barriga C (2016): Removal of heavy metals from simulated wastewater by in situ formation of layered double hydroxides. 306, 1035–1040. *Chem. Eng. J.* <https://doi.org/10.1016/j.cej.2016.08.054>
- Phan T, Bacquet M, Morcellet M (2000) Synthesis and characterization of silica gels functionalized with monochlorotriazinyl β-cyclodextrin and their sorption capacities towards organic compounds. *J Incl Phenom Macrocycl Chem* 38:345–359. <https://doi.org/10.1023/A:1008169111023>
- Rajabi M, Mahanpoor K, Moradi O (2017) Removal of dye molecules from aqueous solution by carbon nanotubes and carbon nanotube functional groups: critical review. *RSC Adv* 7:47083–47090. <https://doi.org/10.1039/C7RA09377B>
- Rajmohan et al., 2020 K Rajmohan R Chandrasekaran S Varjani 2020 A Review on Occurrence of Pesticides in Environment and Current Technologies for Their Remediation and Management *Indian J Microbiol* 1–14 <https://doi.org/10.1007/s12088-019-00841-x>
- Rehman TU, Shah LA, Khan M, Irfan M, Khattak NS (2019) Zwitterionic superabsorbent polymer hydrogels for efficient and selective

- removal of organic dyes. *RSC Adv* 9:18565–18577. <https://doi.org/10.1039/C9RA02488C>
- Reinholds I, Pugajeva I, Zacs D, Lundanes E, Rusko J, Perkons I, Bartkevics V (2017): Determination of acidic non-steroidal anti-inflammatory drugs in aquatic samples by liquid chromatography-triple quadrupole mass spectrometry combined with carbon nanotubes-based solid-phase extraction. *Environ. Monit. Assess.* 189, 568. <https://doi.org/10.1007/s10661-017-6304-9> <https://hrcaj.srce.hr/66125>
- Rochon M-E, Moussa A, Autmizguine J (2019): Antibiotic Considerations for Necrotizing Enterocolitis, Infectious Disease and Pharmacology. Elsevier, pp. 155–166. <https://doi.org/10.1016/B978-0-323-54391-0.00013-8>
- Rojas S, Horcajada PJCR (2020): Metal–Organic Frameworks for the Removal of Emerging Organic Contaminants in Water. <https://doi.org/10.1016/j.ccr.2018.10.003>
- Salman J, Hameed B (2010) Adsorption of 2, 4-dichlorophenoxyacetic acid and carbofuran pesticides onto granular activated carbon. *Desalination* 256:129–135. <https://doi.org/10.1016/j.desal.2010.02.002>
- Sarker M, Ahmed I, Jung SH (2017): Adsorptive removal of herbicides from water over nitrogen-doped carbon obtained from ionic liquid@ ZIF-8. 323, 203–211. *Chem. Eng. J.* <https://doi.org/10.1016/j.cej.2017.04.103>
- Sarker M, Shin S, Jeong JH, Jung SH (2019): Mesoporous metal-organic framework PCN-222 (Fe): Promising adsorbent for removal of big anionic and cationic dyes from water. 371, 252–259. *Chem. Eng. J.* <https://doi.org/10.1016/j.cej.2019.04.039>
- Schreiber B, Wald D, Schmalz V, Worch E (2006): Removal of dissolved organic compounds by granular activated carbon, Chemicals as Intentional and Accidental Global Environmental Threats. Chemicals as Intentional and Accidental Global Environmental Threats. Springer, pp. 397–400. https://doi.org/10.1007/978-1-4020-5098-5_34
- Selvam PP, Preethi S, Basakaralingam P, Thinakaran N, Sivasamy A, Sivanesan S (2008) Removal of rhodamine B from aqueous solution by adsorption onto sodium montmorillonite. *J Hazard Mater* 155:39–44. <https://doi.org/10.1016/j.jhazmat.2007.11.025>
- Seo YS, Khan NA, Jung SH (2015) Adsorptive removal of methylchlorophenoxypropionic acid from water with a metal-organic framework. *Chem Eng J.* <https://doi.org/10.1016/j.cej.2015.02.007>
- Shen Y, Fan C-C, Wei Y-Z, Du J, Zhu H-B, Zhao Y (2016) An anionic zeolite-like metal–organic framework (AZMOF) with a Moravia network for organic dye adsorption through cation-exchange. *Dalton Trans* 45:10909–10915. <https://doi.org/10.1039/C6DT01697A>
- Silva M, Feijão E, de Carvalho RdC, Duarte IA, Matos AR, Cabrita MT, Barreiro A, Lemos MF, Novais SC, Marques JC (2020) Comfortably numb: Ecotoxicity of the non-steroidal anti-inflammatory drug ibuprofen on *Phaeodactylum tricornutum*. *Mar Environ Res* 161:105109. <https://doi.org/10.1016/j.marenvres.2020.105109>
- Sirés I, Guivarch E, Oturan N, Oturan MA (2008) Efficient removal of triphenylmethane dyes from aqueous medium by in situ electro-generated Fenton's reagent at carbon-felt cathode. *Chemosphere* 72:592–600. <https://doi.org/10.1016/j.chemosphere.2008.03.010>
- Sivamani S, Leena G (2009) Removal of dyes from wastewater using adsorption-a review. *Int J Biosci Technol* 2:47–51
- Song Y, Ma R, Hao L, Yang X, Wang C, Wu Q, Wang Z (2018) Application of covalent organic framework as the adsorbent for solid-phase extraction of trace levels of pesticide residues prior to high-performance liquid chromatography-ultraviolet detection. *J Chromatogr A* 1572:20–26. <https://doi.org/10.1016/j.chroma.2018.08.033>
- Song Y, Sun Q, Aguila B, Ma S (2019) Opportunities of covalent organic frameworks for advanced applications. *Adv Sci* 6:1801410. <https://doi.org/10.1002/advs.201801410>
- Stuart M, Lapworth D (2013): Emerging organic contaminants in groundwater, Smart Sensors for Real-Time Water Quality Monitoring. Smart Sensors for Real-Time Water Quality Monitoring. Springer, pp. 259–284. https://doi.org/10.1007/978-3-642-37006-9_12
- Sun Y, Chen J, Li A, Liu F, Zhang Q (2005) Adsorption of resorcinol and catechol from aqueous solution by aminated hypercrosslinked polymers. *React Funct Polym* 64:63–73. <https://doi.org/10.1016/j.reactfunctpolym.2005.03.004>
- Suresh S, Srivastava VC, Mishra I (2011): Study of catechol and resorcinol adsorption mechanism through granular activated carbon characterization, pH and kinetic study. 46, 1750–1766. *Sep Sci Technol.* <https://doi.org/10.1080/01496395.2011.570284>
- Tan JZ, Nursam NM, Xia F, Sani M-A, Li W, Wang X, Caruso R (2017) High-performance coral reef-like carbon nitrides: synthesis and application in photocatalysis and heavy metal ion adsorption. *ACS Appl Mater Interfaces* 9:4540–4547. <https://doi.org/10.1021/acsami.6b11427>
- Vyavahare GD, Gurav RG, Jadhav PP, Patil RR, Aware CB, Jadhav JP (2018) Response surface methodology optimization for sorption of malachite green dye on sugarcane bagasse biochar and evaluating the residual dye for phyto and cytogenotoxicity. *Chemosphere* 194:306–315. <https://doi.org/10.1016/j.chemosphere.2017.11.180>
- Walcarius A, Mercier L (2010) Mesoporous organosilica adsorbents: nanoengineered materials for removal of organic and inorganic pollutants. *J Mater Chem* 20:4478–4511. <https://doi.org/10.1039/B924316J>
- Wang F, Yao J, Sun K, Xing B (2010) Adsorption of dialkyl phthalate esters on carbon nanotubes. *Environ Sci Technol* 44:6985–6991. <https://doi.org/10.1021/es101326j>
- Wang H, Guo H, Zhang N, Chen Z, Hu B, Wang X (2019) Enhanced photoreduction of U (VI) on C₃N₄ by Cr (VI) and bisphenol A: ESR, XPS, and EXAFS investigation. *Environ Sci Technol* 53:6454–6461. <https://doi.org/10.1021/acs.est.8b06913>
- Wang J, Bai Z (2017) Fe-based catalysts for heterogeneous catalytic ozonation of emerging contaminants in water and wastewater. *Chem Eng J* 312:79–98. <https://doi.org/10.1016/j.cej.2016.11.118>
- Wang J, Wang S (2018a) Microbial degradation of sulfamethoxazole in the environment. *Appl Microbiol Biotechnol* 102:3573–3582. <https://doi.org/10.1007/s00253-018-8845-4>
- Wang J, Wang S (2018): Activation of persulfate (PS) and peroxy-monosulfate (PMS) and application for the degradation of emerging contaminants. 334, 1502–1517. *Chem. Eng. J.* <https://doi.org/10.1016/j.cej.2017.11.05>
- Wang J, Wang S (2019) Preparation, modification and environmental application of biochar: a review. *J Clean Prod* 227:1002–1022. <https://doi.org/10.1007/s11356-018-3368-1>
- Wang K, Yang LM, Wang X, Guo L, Cheng G, Zhang C, Jin S, Tan B, Cooper A (2017) Covalent triazine frameworks via a low-temperature polycondensation approach. *Angew Chem* 56:14149–14153. <https://doi.org/10.1002/anie.201708548>
- Wang RQ, Wei XB, Feng YQ (2018a) β -Cyclodextrin covalent organic framework for selective molecular adsorption. *Chem Eur J* 24:10979–10983. <https://doi.org/10.1021/acs.omega.9b03176>
- Wang S, Li D, Sun C, Yang S, Guan Y, He H (2014a) Synthesis and characterization of g-C₃N₄/Ag₃VO₄ composites with significantly enhanced visible-light photocatalytic activity for triphenylmethane dye degradation. *Chemosphere* 144:885–892. <https://doi.org/10.1016/j.chemosphere.2008.03.010>
- Wang T, Kailasam K, Xiao P, Chen G, Chen L, Wang L, Li J, Zhu J (2014b) Adsorption removal of organic dyes on covalent triazine framework (CTF). *Microporous Mesoporous Mater* 187:63–70. <https://doi.org/10.1016/j.micromeso.2013.12.016>

- Wang W, Deng S, Ren L, Li D, Wang W, Vakili M, Wang B, Huang J, Wang Y, Yu G (2018b) Stable covalent organic frameworks as efficient adsorbents for high and selective removal of an aryl-organophosphorus flame retardant from water. *ACS Appl Mater Interfaces* 10:30265–30272. <https://doi.org/10.1021/jacs.7b02696>
- Wei et al., 2020a D Wei J Li Z Chen L Liang J Ma M Wei Y Ai X Wang 2020a Understanding bisphenol-A adsorption in magnetic modified covalent organic frameworks: Experiments coupled with DFT calculations *J Mol Liq* 112431 <https://doi.org/10.1016/j.molliq.2019.112431>
- Wei D, Li J, Chen Z, Liang L, Ma J, Wei M, Ai Y, Wang X (2020b) Understanding bisphenol-A adsorption in magnetic modified covalent organic frameworks: Experiments coupled with DFT calculations. *J Mol Liq* 301:112431. <https://doi.org/10.1016/j.molliq.2019.112431>
- Wei W, Sun R, Cui J, Wei Z (2010) Removal of nitrobenzene from aqueous solution by adsorption on nanocrystalline hydroxyapatite. *Desalination* 263:89–96. <https://doi.org/10.1016/j.desal.2010.06.043>
- Wen A, Li G, Wu D, Yu Y, Yang Y, Hu N, Wang H, Chen J, Wu Y (2020) Sulphonate functionalized covalent organic framework-based magnetic sorbent for effective solid phase extraction and determination of fluoroquinolones. *J Chromatogr A* 1612:460651. <https://doi.org/10.1016/j.chroma.2019.460651>
- Wong KT, Yoon Y, Snyder SA, Jang M (2016) Phenyl-functionalized magnetic palm-based powdered activated carbon for the effective removal of selected pharmaceutical and endocrine-disruptive compounds. *Chemosphere* 152:71–80. <https://doi.org/10.1016/j.chemosphere.2016.02.090>
- Xing Z, Tian J, Liu Q, Asiri AM, Jiang P, Sun X (2014) Holey graphene nanosheets: large-scale rapid preparation and their application toward highly-effective water cleaning. *Nanoscale* 6:11659–11663. <https://doi.org/10.1039/C4NR03104K>
- Xu et al., 2020 S-X Xu Z-Q Yao Y-H Zhang 2020 A covalent organic framework exhibiting amphiphilic selective adsorption toward ionic organic dyes tuned by pH value *Eur Polym J* 109764 <https://doi.org/10.1016/j.eurpolymj.2020.109764>
- Xu Y, Liu T, Zhang Y, Ge F, Steel RM, Sun L (2017) Advances in technologies for pharmaceuticals and personal care products removal. *J Mater Chem a* 5:12001–12014. <https://doi.org/10.1039/C7TA03698A>
- Xue H, Chen Q, Jiang F, Yuan D, Lv G, Liang L, Liu L, Hong MJC, (2016) A regenerative metal–organic framework for reversible uptake of Cd (ii): from effective adsorption to in situ detection. *Chem Sci J* 7:5983–5988. <https://doi.org/10.1039/C6SC00972G>
- Yang Y, Ok YS, Kim K-H, Kwon EE, Tsang YF (2017) Occurrences and removal of pharmaceuticals and personal care products (PPCPs) in drinking water and water/sewage treatment plants: A review. *Sci Total Environ* 596:303–320. <https://doi.org/10.1016/j.scitotenv.2017.04.102>
- Yao Y, Mi N, Zhu Y, Yin L, Zhang Y, Li S (2019) Efficient removal of sulfamerazine (SMR) by ozonation in acetic acid solution after enrichment SMR from water using granular activated carbon. *RSC Adv* 9:9145–9152. <https://doi.org/10.1039/C8RA10429H>
- Ye J, Jin L, Zhao X, Qian X, Dong M (2019) Superior adsorption performance of metal-organic-frameworks derived magnetic cobalt-embedded carbon microrods for triphenylmethane dyes. *J Colloid Interface Sci* 536:483–492. <https://doi.org/10.1016/j.jcis.2018.10.073>
- You L, Nguyen VT, Pal A, Chen H, He Y, Reinhard M, Gin KY-H (2015) Investigation of pharmaceuticals, personal care products and endocrine disrupting chemicals in a tropical urban catchment and the influence of environmental factors. *Sci Total Environ* 536:955–963. <https://doi.org/10.1016/j.scitotenv.2015.06.041>
- Yu S-B, Lyu H, Tian J, Wang H, Zhang D-W, Liu Y, Li Z-T (2016) A polycationic covalent organic framework: a robust adsorbent for anionic dye pollutants. *Polym Chem* 7:3392–3397. <https://doi.org/10.1039/C6PY00281A>
- Yusuf M, Elfghi F, Zaidi SA, Abdullah E, Khan MA (2015) Applications of graphene and its derivatives as an adsorbent for heavy metal and dye removal: a systematic and comprehensive overview. *RSC Adv* 5:50392–50420. <https://doi.org/10.1039/C5RA07223A>
- Zahoor M, Mahramanlioglu M (2011): Adsorption of imidacloprid on powdered activated carbon and magnetic activated carbon. *Chem Biochem Eng Q.* 25, 55–63. <https://hrcak.srce.hr/66125>
- Zhang C, Zhu P-C, Tan L, Liu J-M, Tan B, Yang X-L, Xu H-B (2015) Triptycene-based hyper-cross-linked polymer sponge for gas storage and water treatment. *Macromolecules* 48:8509–8514. <https://doi.org/10.1021/acs.macromol.5b02222>
- Zhang H, Fang D, Kong Z, Wei J, Wu X, Shen S, Cui W, Zhu Y (2018a): Enhanced adsorption of phthalic acid esters (PAEs) from aqueous solution by alkylbenzene-functionalized polypropylene nonwoven and its adsorption mechanism insight. 331, 406–415. *Chem. Eng. J.* <https://doi.org/10.1016/j.cej.2017.07.144>
- Zhang Q, Yu J, Cai J, Song R, Cui Y, Yang Y, Chen B, Qian G (2014) A porous metal–organic framework with–COOH groups for highly efficient pollutant removal. *Chem Comm* 50:14455–14458
- Zhang W, Zhang L, Zhao H, Li B, Ma H (2018b) A two-dimensional cationic covalent organic framework membrane for selective molecular sieving. *J Mater Chem a* 6:13331–13339. <https://doi.org/10.1039/C4CC06648K>
- Zhou M, Wu HB, Ren G, Li MY (2011): Study of control for phenol and chlorophenols sudden pollution in drinking water by using PAC adsorption. *Adv Mat Res.* pp. 2410–2413. 4028/www.scientific.net/AMR.236-238.2410
- Zhu X, An S, Liu Y, Hu J, Liu H, Tian C, Dai S, Yang X, Wang H, Abney C (2017) Efficient removal of organic dye pollutants using covalent organic frameworks. *AIChE J* 63:3470–3478. <https://doi.org/10.1002/aic.15699>
- Zhuan R, Wang J (2019) Degradation of sulfamethoxazole by ionizing radiation: Kinetics and implications of additives. *Sci Total Environ* 668:67–73. <https://doi.org/10.1016/j.scitotenv.2019.03.027>
- Zhuang S, Zhu X, Wang J (2018) Kinetic, equilibrium, and thermodynamic performance of sulfonamides adsorption onto graphene. *Environ Sci Pollut Res* 25:36615–36623
- Zhuang S, Chen R, Liu Y, Wang J (2020a) Magnetic COFs for the adsorptive removal of diclofenac and sulfamethazine from aqueous solution: Adsorption kinetics, isotherms study and DFT calculation. *J Hazard Mater* 385:121596. <https://doi.org/10.1016/j.jhazmat.2019.121596>
- Zhuang S, Liu Y, Wang J (2020b) Covalent organic frameworks as efficient adsorbent for sulfamerazine removal from aqueous solution. *J Hazard Mater* 383:121126. <https://doi.org/10.1016/j.jhazmat.2019>
- Zhuang X, Wan Y, Feng C, Shen Y, Zhao D (2009) Highly efficient adsorption of bulky dye molecules in wastewater on ordered mesoporous carbons. *Chem Mater* 21:706–716. <https://doi.org/10.1021/cm8028577>
- Гыцак ВВ, Лышак ВІ (2018): Pesticide Toxicity: A Mechanistic Approach. *EXCLI J* 17:1101–1136. <https://doi.org/10.17179/excli.2018-1710>

Publisher's note Springer Nature remains neutral with regard to jurisdictional claims in published maps and institutional affiliations.